



MARIA CURIE-SKŁODOWSKA
UNIVERSITY, LUBLIN
LUBLIN UNIVERSITY
OF TECHNOLOGY
POLISH PHYSICAL SOCIETY

XIII-th INTERNATIONAL CONFERENCE

**ION IMPLANTATION
AND OTHER APPLICATIONS
OF IONS AND ELECTRONS**

ION 2022

**Kazimierz Dolny, Poland
June 27-30, 2022**

XIII-th INTERNATIONAL CONFERENCE

on

ION IMPLANTATION AND OTHER APPLICATIONS OF IONS AND ELECTRONS



**June 27-30, 2022
Kazimierz Dolny, Poland**

Edited by
Janusz Filiks, Marcin Turek and Jerzy Żuk



The conference is supported by the Ministry of Science and Higher Education of the Republic of Poland in the frame of the Project "Excellent Science - Support of Scientific Conferences"

The Market Square in Kazimierz Dolny drawn by Artur Orłowski

CHAIRPERSONS

Jerzy Żuk – chairman, Maria Curie-Skłodowska University

Marcin Turek – co-chairman, Maria Curie-Skłodowska University

Paweł Żukowski – co-chairman, Lublin University of Technology

INTERNATIONAL SCIENTIFIC COMMITTEE

Michał Boćkowski (Poland)

Piotr Budzyński (Poland)

Jacek Jagielski (Poland)

Fadei F. Komarov (Belarus)

Tomasz Kołtunowicz (Poland)

Alexander D. Pogrebnyak (Ukraine)

Sławomir Prucnal (Germany, Poland)

Wolfgang Skorupa (Germany)

Bronisław Słowiński (Poland)

Lionel Thomé (France)

Andrzej Turoś (Poland)

Zbigniew Werner (Poland)

Paweł Węgierek (Poland)

Shengqiang Zhou (Germany)

LOCAL ORGANIZING COMMITTEE

Janusz Filiks (Secretary – Maria Curie-Skłodowska University)

Andrzej Drożdżel (Maria Curie-Skłodowska University)

Mirosław Kulik (Maria Curie-Skłodowska University)

Krzysztof Pysznik (Maria Curie-Skłodowska University)

Mirosław Szala (Lublin University of Technology)

Marcin Turek (Maria Curie-Skłodowska University)

CONTENTS

SPECIAL LECTURES

- SL-1 *Domański Tadeusz*, Synergy of semiconductor physics and electron pairing: route towards novel topological materials.....11
- SL-2 *Jasińska Bożena*, New method of imaging in PET based on morphometric indicator.....12

INVITED LECTURES

- I-1 *Bockowski M.*, Innovative approach for changing electrical and optical properties of GaN.....15
- I-2 *Czerski K., Dubey R., Kaczmarek M., Kowalska A., Targosz-Sleczka N., Valat M.*, How do crystal lattice defects increase nuclear fusion reaction rates?.....16
- I-3 *Guziewicz M., Wzorek M., Piskorski K., Pagowska K., Czuba K., Myśliwiec M., Juchniewicz M., Jakiela R., Domagala J.*, Characterization of SiC 4H films formed by Al or N implantation, and thermal activation for power devices17
- I-4 *Horodek P., Siemek K., Mirzayev M.N., Donkov A.A., Popov E.P., Kulik M. and Turek M.*, Defects studies of gold exposed to Au and H implantation.....19
- I-5 *Jagielski Jacek, Nowicki Lech, Mieszczyński Cyprian, Skrobos Kazimierz, Jóźwik Przemysław, Jóźwik Iwona, Thomé Lionel, Garrido Frédéric, Gentils Aurelie*, McChasy 2; a new Monte Carlo simulation code designed for a use with large atomic structures.....20
- I-6 *Jóźwik I., Jagielski J., Dumiszewska E., Kamiński P., Caban P. and Kentsch U.*, Ion-irradiated damage-induced resistivity contrast imaging of semiconductor structures with ultra-low energy electrons21
- I-7 *Komarov F., Vlasukova L., Makhavikou M., Parkhomenko I., Yuvchenko V., Milchanin O., Dauletbekova A., Żuk J., Janse van Vuren F., Neethling J.*, Swift heavy ion modification of A₃B₅ nanoparticles and zinc- based core- shell nanostructures embedded in silica.....23
- I-8 *Kozanecki A., Sajkowski J.M., Mathew J.A., Zhydachevskyy Y., Alves E. and Stachowicz M.*, Europium implanted ZnO-based quantum structures.....24
- I-9 *O'Connell J. and Douglas-Henry D.*, SHI induced bulk rotation in non-amorphizable targets25
- I-10 *Pelc Andrzej*, Negative ion formation by low energy electron interaction with molecules26
- I-11 *Pęczkowski Paweł*, Influence of noble gas ions irradiation on the structural and magnetic properties of HTS-2G tapes27
- I-12 *Prucnal Sławomir*, Defect engineering in degenerate semiconductors using intense pulsed light28

I-13	<i>Ratajczak Renata, Guzewicz Elżbieta, Prucnal Sławomir, Mieszczynski Cyprian, Jozwik Przemysław, Turows Andrzej, Krajewski Tomasz A., Wozniak Wojciech, Wierzbicka Aleksandra, Heller Rene, Kentsch Ulrich, Facsko Stefan,</i> Comprehensive approach to the studies of Zinc Oxide implanted with rare-earth ions for future optoelectronic device applications	29
I-14	<i>Sartowska B., Barlak M., Starosta W., Waliś L., Smolik J.,</i> Surface modification of zirconium alloys used for claddings to improve the corrosion resististance	31

ORAL PRESENTATIONS

O-1	<i>Janse van Vuuren Arno, Ibrayeva Anel, Skuratov Vladimir, Zdorovets Maxim,</i> Microstructural response of silicon nitride to fission fragments	35
O-2	<i>Kulik M., Kołodyska D., Żuk J., Hubicki Z. and Turek M.,</i> Optical spectra and chemical composition of native oxide layers on hot-implanted GaAs	36
O-3	<i>Szala M., Chocyk D., Turek M., Skic A.,</i> Effect of nitrogen ion implantation on cavitation erosion resistance of CoCrWC alloy	37
O-4	<i>Turek M., Drożdżel A., Pysznik K., Grudziński W., Węgierek P.,</i> Modification of PET foil properties by 150 keV Li ⁺ ion implantation	38
O-5	<i>Yastrubchak O., Tataryn N., Wosinski T., Sadowski J., Domagala J.Z., Sawicki M., Gluba L. and Żuk J.,</i> Multicomponent dilute ferromagnetic semiconductors on the base of (Ga,Mn)As for spintronic applications	39

YOUNG SCIENTISTS CONTEST

Oral presentations

YSC-1	<i>Ibrayeva A., O'Connell J., Mutali A., Korneeva E., Sohatsky A. and Skuratov V.,</i> Tolerance of nanocrystalline Y ₄ Al ₂ O ₉ for SHI irradiation	43
YSC-2	<i>Jaroszyński P., Grzanka E., Grabowski M., Jakiela R., Sierakowski K., Prozheev I., Tuomisto F., Boćkowski M.,</i> Ultra-high pressure doping of GaN with europium	44
YSC-3	<i>Jóźwik P., Mieszczynski C., Skrobias K., Ratajczak R., Jagielski J., Garrido F., Alves E., Lorenz K.,</i> Modeling of dislocations and dislocation loops for Monte Carlo simulations of ion channeling.....	45
YSC-4	<i>Krutul K.Z., Horodek P., Napiorkowski P.J., Hadyńska-Klęk K., Komorowska M., Olejniczak A., Paluch-Ferszt M., Siemek K., Szepliński Z., Wróbel M., Wrzosek-Lipska K.,</i> Radiation resistance studies of PIN diode detectors irradiated with heavy ions	46
YSC-5	<i>Lech M., Węgierek P. and Turek M.,</i> Physical aspect of initiation and development of discharges in vacuum interrupters used in electric power switchgear	47
YSC-6	<i>Li Yi, Steuer Oliver, Lin Kaiman, Helm Manfred, Zhou Shengqiang and Prucnal Sławomir,</i> Modification of two-dimensional materials using ion implantation.....	48

YSC-7	<i>Sarwar Mahwish, Ratajczak Renata, Ivanov Vitalii, Mishra Sushma, Turek Marcin, Guziewicz Elzbieta</i> , Crystal lattice damage and recovery of rare-earth implanted wide bandgap oxides	50
YSC-8	<i>Sierakowski K., Jakiela R., Sochacki T., Iwinska M., Jaroszynski P. Fijalkowski M., Turek M., and Bockowski M.</i> , Investigation of beryllium diffusion for various crystallographic directions in GaN grown by HVPE	52

Poster presentation

YSC-9	<i>Gawęda M., Wilczopolska M., Suchorab K., Frelek-Kozak M., Kurpaska Ł., Józwiak I., Jagielski J.</i> , Structural degradation in graphite after argon ion irradiation investigated with Raman imaging	53
-------	---	----

POSTER PRESENTATIONS

Po-1	<i>Budzyński P., Kamiński M., Surowiec M., Turek M., Wiertel M., Skuratov V.A.</i> , The effect of carbon ion implantation and xenon irradiation on tribological properties of titanium and Ti6Al4V alloy	57
Po-2	<i>Horodek P., Siemek K., Skuratov V.A.</i> , Defects studies of gold exposed to Au and H implantation	58
Po-3	<i>Gałaszkiwicz P. and Koltunowicz T.N.</i> , AC conductivity of Ti-Zr-C hard nanocomposite coatings	59
Po-4	<i>Komarov Fadei F., Konstantinov Stanislav V., Żuk Jerzy, Chizhov Igor V., Zaikov Valery A.</i> , TiAlN coatings blistering under high-temperature Ar ⁺ ion irradiation	60
Po-5	<i>Szala Mirosław, Kamiński Mariusz, Łatka Leszek</i> , Effect of atmospheric plasma spraying parameters on cavitation erosion and wet-environment tribological behaviour of Al ₂ O ₃ -13% TiO ₂ coatings	61
Po-6	<i>Phuc T.V., Kulik M., Khiem L.H., Tuan P.L., Tiep N.V., Tuyen L.A., Doroshkevich A., Madadzada Afag</i> , Influence of energy and mass of ion on TiO ₂ /SiO ₂ bilayer mixing.....	62
Po-7	<i>Kucal E., Czerski K., Koziol Z.</i> , Molecular dynamics simulations of primary radiation damage in Silicon Carbide	63
Po-8	<i>Lee M.E., O'Connell J. and Skuratov V.</i> , Orientation dependence of RT stabilized SHI induced tetragonal tracks in a ZrO ₂ monoclinic matrix	64
Po-9	<i>Ksenevich V.K., Dorosinets V.A., Adamchuk D.V., Samarina M.A., Lyubchyk A.I.</i> , Structure and magnetic properties of Ni-doped tin oxide films.....	65
Po-10	<i>Makhavikou Maksim, Komarov Fadei, Komarov Alexandr, Miskevich Sergei, Milchanin Oleg, Parkhomenko Irina, Żuk Jerzy, Romanov Ivan and Wendler Elke</i> , Formation of ZnSe nanoclusters in silicon dioxide layers by high-fluence ion implantation: Experimental data and simulation results.....	66
Po-11	<i>Miskiewicz S., Komarov A., Komarov F.</i> , Simulation of coimplantation of boron and carbon in silicon.....	67

Po-12	<i>Nagornyi A.V., Shlapa Yu.Yu., Belous A.G., Vekas L., Bulavin L.A.</i> , Structural ordering of magnetic nanoparticles in aqueous media by small-angle neutron scattering	68
Po-13	<i>Pogrebnjak A.D., Ivashchenko V.I., Budzyński P., Kamiński M.</i> , Microstructure, chemical bonding and tribo-mechanical properties of Ti-Zr-Mo-C.....	69
Po-14	<i>Popov E.P., Mirzayev M.N., Donkov A.A., Hussien M.A.M., Obiedallah F.M.H., Anatolievich S.A., Horodek Paweł</i> , First-principles study of defect formation and migration in nano size TiC crystal under ions irradiation	70
Po-15	<i>Sierakowski K., Jakiela R., Sochacki T., Iwinska M., Jaroszynski P., Fijalkowski M., Turek M., and Bockowski M.</i> , Investigation of zinc diffusion for various crystallographic directions in GaN grown by HVPE.....	71
Po-16	<i>Szala Mirosław, Turek Marcin, Chocyk Dariusz, Skic Anna</i> , Effect of nitrogen ion implantation on cavitation erosion resistance of Stellite 12 and Stellite 6 hardfacings.....	73
Po-17	<i>Turek M.</i> , Ionization in hot cavity ion sources	74
Po-18	<i>Turek M.</i> , Ionization of short-lived nuclides in a hot disc-shaped cavity.....	75
Po-19	<i>Musiatowicz M., Turek M., Drożdźiel A., Pysznik K., Grudziński W.</i> , Modification of optical electronic and microstructural properties of PET by 150 keV Cs ⁺ irradiation.....	76
Po-20	<i>Turek M., Drożdźiel A., Pysznik K.</i> , New approach to non-volatile metal ion production using plasma ion source with internal evaporator.....	77
Po-21	<i>Turek M., Węgierek P.</i> , Suppressing of co-extracted electrons in a negative ion source-numerical simulations.....	78
Po-22	<i>Turek M., Drożdźiel A., Pysznik K., Węgierek P.</i> , Thermal desorption of Ar implanted into GaAs	79
Po-23	<i>Turek M., Drożdźiel A., Pysznik K., Prucnal S., Węgierek P.</i> , Thermal desorption of Kr implanted into germanium	80
Po-24	<i>Valizade A.H., Mirzayev M.N., Samedov O.A., Siemek Krzysztof</i> , Surface processes under the influence of Xe ion irradiation with 167 MeV energy in tungsten-based compounds	81
Po-25	<i>Walczak Mariusz, Pasierbiewicz Kamil, Szala Mirosław</i> , Effect of Ti6Al4V substrate manufacturing technology on properties of PVD nitride coatings.....	82
Po-26	<i>Winiarczyk K., Surowiec Z., Góral-Kowalczyk M., Gac W.</i> , Magnetite nanoparticles modified with organic compounds.....	83
	Authors Index.....	85

SPECIAL LECTURE

SPECIAL LECTURE (SL-1)

Synergy of semiconductor physics and electron pairing: route towards novel topological materials

Domański Tadeusz

M. Curie-Skłodowska University, 20-031 Lublin, Poland

Electrons moving through a crystal lattice, according to the Bloch theorem, are characterized by the band spectrum. Upon introducing a certain amount of local defects (impurities) such gapped electronic structure is modified by the acceptor and/or donor bound states appearing between the valence and conduction bands, which substantially enhance electronic conductance of the doped semiconductors.

An analogous process can be also realized in isotropic superconductors, where the electron pairing prohibits any single-particle states to exist around the Fermi energy in clean samples. In presence of the magnetic impurities, which can be regarded as 'pair-breakers', there emerge the resonant (Shiba) states inside the pairing gap. Their signatures have been reported, both by the ballistic charge tunneling experiments and the high-resolution scanning spectroscopy.

During the recent decade a great deal of interest has been devoted to magnetic chains (of nanoscopic length) deposited on superconducting substrates and/or semiconducting nanowires (e.g. InSb) contacted with superconducting leads, where the Shiba states undergo a qualitative evolution, developing the topologically nontrivial phase [1]. In analogy to topological insulators they are characterized by exotic boundary quasiparticles, here reminiscent of the Majorana fermions [2]. By virtue of topological protection such boundary modes are perfect candidates for constructing the quantum bits and for designing unconventional logic operations of quantum computers. I shall briefly overview the current status on such topological structures.

References

- [1] K. Laubscher and J. Klinovaja, Majorana bound states in semiconducting nanostructures, *Journal of Applied Physics* 130, 081101 (2021).

SPECIAL LECTURE (SL-2)

New method of imaging in PET based on morphometric indicator

*Jasińska Bożena**

for J-PET collaboration

Institute of Physics, Maria Curie Skłodowska University, 20-031 Lublin, Poland

Two the most known techniques based on positron-electron annihilation are PET (Positron Emission Tomography) and PALS (Positron Annihilation Lifetime Spectroscopy).

PET is a diagnostic method enabling imaging of the metabolism of chosen substances in the living organism. Metabolism rate depends on many factors, one of them is cancer growth in some region of body.

Other technique, commonly used in material sciences, PALS, allows following precisely kind of processes leading to positron annihilation, including creation and decaying the positronium (bound state of positron-electron) states. It is known that o-Ps lifetime value reflects size of the free spaces in which it is trapped. Then, one can expect it can be used to investigate tissue modification during some kind of diseases. Additionally, intensity of this component allows to follow charge activity of some processes, including cell apoptosis or radical creation. The proposed parameter δ brings together both, lifetime and intensity value. It can be included to PET as a new imaging method reflecting morphometric changes in human body.

Preliminary investigation performed on real healthy and altered human tissues using PALS clearly indicates that it is possible to distinguish between healthy and diseased tissues and between different kinds of lesions of the some organ using techniques based on positron annihilation.

* email: bozena.jasinska@umcs.pl

INVITED LECTURE

Innovative approach for changing electrical and optical properties of GaN

Bockowski M.

Institute of High Pressure Physics PAS, Sokolowska 29/37, 01-142 Warsaw, Poland

It is well known that nitride semiconductors based on gallium nitride (GaN) and its cousins, indium nitride (InN) and aluminum nitride (AlN), are applied for building light emitting diodes, laser diodes as well as high-power and high-frequency transistors. These devices are used in many fields from general lighting, medicine through ecology up to defense. Although nitride-based devices show tremendous technological promise, their reliability and commercial success can still be improved by higher structural quality of crystallized material as well as more homogeneous and precise doping by donors and acceptors.

One of the best methods for introducing dopants into semiconductors is ion implantation. The introduced structural damage can be removed by a proper annealing process. The high-temperature treatment enables also electrical and/or optical activation of the implanted dopants. In the case of GaN, annealing at high temperature ($\sim 1300^{\circ}\text{C}$ - 1400°C) seems difficult. This compound loses its thermodynamic stability slightly above 800°C at atmospheric pressure. At higher temperature the crystal will decompose. One of the solutions is to anneal GaN at high nitrogen (N_2) pressure. Such technology is called ultra-high-pressure annealing (UHPA).

In this paper, application of UHPA for GaN crystals and layers implanted by different ions (acceptors and donors) will be presented. The latest results of the implantation with magnesium (Mg), beryllium (Be), zinc (Zn), and calcium (Ca) ions into GaN in order to obtain p-type conductivity will be discussed. Silicon (Si) implantation into GaN for n-type doping will also be analyzed. Structural, electrical and optical properties of implanted GaN after UHPA will be discussed in terms of application for GaN-based devices.

How do crystal lattice defects increase nuclear fusion reaction rates?

Czerski K.^{1)*}, *Dubey R.*¹⁾, *Kaczmarek M.*¹⁾, *Kowalska A.*²⁾, *Targosz-Slecza N.*¹⁾,
*Valat M.*¹⁾

¹ *Institute of Physics, University of Szczecin, 70-451 Szczecin, Poland*

² *Physics Department, Maritime University of Szczecin, 70-500 Szczecin, Poland*

Recent studies of the deuteron-deuteron nuclear reactions in metallic targets, at projectile energies far below the Coulomb barrier, show a significant enhancement of cross sections due to the electron screening effect and the threshold resonance contribution. Both effects are sensitive to the crystal lattice defects of the target material which increases the effective electron mass. Based on experimental results and the atomic deuteron-deuteron potential, we could calculate the cross section of $^2\text{H}(\text{d},\text{p})^3\text{H}$ reaction and the e-e+ pair production down to energies corresponding to room temperature where the enhancement effects are of crucial importance. We also demonstrate the commercial applicability of the new energy source.

* konrad.czerski@usz.edu.pl

Characterization of SiC 4H films formed by Al or N implantation, and thermal activation for power devices

Guziewicz M.¹⁾, Wzorek M.¹⁾, Piskorski K.¹⁾, Pagowska K.¹⁾, Czuba K.¹⁾, Myśliwiec M.²⁾, Juchniewicz M.²⁾, Jakiela R.³⁾, Domagala J.³⁾

¹⁾Lukasiewicz Research Network – Institute of Microelectronics and Photonics – Warsaw

²⁾CEZAMAT – Warsaw University of Technology – Warsaw

³⁾Institute of Physics, Polish Academy of Science – Warsaw

Fabrication of SiC power semiconductor devices like Insulated Gate Bipolar Transistors (IGBT) or MOSFETs requires formation of p/n junctions by using ion implantation. Such method allows to form p- and n-type regions in SiC crystal with controlled concentration of dopants depths due to accurate control of both dose and element ions energy used in implantation process. Typically, the N or P ions are used for donor doping, and Al or B ions are used as acceptor dopants. Unfortunately, ion implantation causes strong damages in the crystal. Post-implantation annealing processes at temperature range from 1600°C to 2000°C are applied to activate dopants and to recover crystal structure. Such thermal processes are complex, and crucial to ensure high activation ratio of dopants and good electrical mobility of carriers in channel of the transistor. Despite various known experimental results in this field from literature [1] there is no conventional process procedure for Al or N dopants activations in SiC. Our studies on implantation and activation of Al and N dopants aim to build up active regions of base, source and channel in a IGBT structure. XRD, TEM, SIMS and Raman spectroscopy methods have been applied in the investigations.

The 4H SiC(0001) substrates were implanted using: Al⁺ ions with 250 keV energy and a dose of $3 \times 10^{14} \text{ cm}^{-2}$, at temperature of 500°C; N²⁺ ions, where multiple implantation process with 10÷75 keV energy and the dose of $1.46 \times 10^{15} \text{ cm}^{-2}$ was performed to form rectangular doping profile. The samples were protected by graphite like coating, next annealed in Ar at temperature in the range of 1600÷1800°C for 30 min. Raman scattering spectra were collected at room temperature using micro-Raman spectrometer UV (266 nm) lasers as excitation sources. Crystal structure of the films was studied by high resolution XRD and TEM methods. Electrical parameters of the films were measured by Hall method.

The amorphous layer is formed near the SiC surface by Al implantation and this is characterized by Raman bands at $\sim 500 \text{ cm}^{-1}$ and $\sim 800 \text{ cm}^{-1}$ for Si-Si and Si-C vibrations, respectively. After the post implantation annealing performed at temperature of 1600°C or above the crystal lattice of 4H-SiC was recovered, although some crystal defects are present, as it was evidenced in the sample annealed at 1800°C by TEM studies. SIMS measurements of concentration profiles for the samples before and after post-implantation annealing show very similar dependences. The crystal quality improves with increasing annealing temperatures. An increasing dependence of normalized Raman A1(LA), E2(TO), and A1(LO) peaks intensities on annealing temperature was found for Al⁺ implanted and next annealed samples up to 1800°C. Similar conclusion

was established based on analysis of HRXRD results for measurement of 00.4SiC reflection on a distorted near surface region.

Acknowledgement

This work was supported by the Polish National Centre for Research and Development (NCBiR) under the project TECHMATSTRATEG within the framework “Modern material technologies”, grant No. 1/347452/1/NCBR/2017.

References

- [1] M.H. Weng, F. Roccaforte, F. Giannazzo, S. Di Franco, C. Bongiorno, M.Saggio, V. Raineri, Mat. Scie. Forum 645, p. 713-716 (2010)

Defects studies of gold exposed to Au and H implantation

Horodek P.¹⁾, Siemek K.¹⁾, Mirzayev M.N.^{2,3)}, Donkov A.A.⁴⁾, Popov E.P.^{4,5)}, Kulik M.⁶⁾ and Turek M.⁶⁾

¹⁾*Institute of Nuclear Physics, Polish Academy of Science, Krakow 31-342, Poland,*

²⁾*Institute of Radiation Problems, Azerbaijan National Academy of Sciences, Baku, AZ1143, Azerbaijan*

³⁾*Azerbaijan State Oil and Industry University, Scientific-Research Institute Geotechnological Problems of Oil, Gas and Chemistry, AZ1010 Baku, Azerbaijan*

⁴⁾*Georgi Nadjakov Institute of Solid State Physics, Bulgarian Academy of Sciences, 1784, Sofia, Bulgaria*

⁵⁾*Institute for Nuclear Research and Nuclear Energy, Bulgarian Academy of Sciences, Sofia, 1784, Bulgaria*

⁶⁾*Institute of Physics, Maria Curie-Skłodowska University, Pl. Marii Curie-Skłodowskiej 1, 20-031 Lublin, Poland*

The interaction of materials with energetic ions is interesting from theoretical and experimental points of view. The changes induced by ions are irreversible at the atomic level and affect significantly material properties.

Within this presentation we report experimental studies performed for pure gold samples exposed to 100 keV self- and 250 keV H⁺ implantation. Radiation damages were investigated with positron annihilation spectroscopy. The Doppler broadening tests obtained with variable energy positron beam show the presence of vacancy-type defects and the filling of the Au vacancies by H. The conventional positron lifetime measurements allow estimating the kind of introduced defects as single vacancies. The pinholes and bubbles formation mechanism has been simulated using molecular dynamics method the SEM analysis.

McChasy 2; a new Monte Carlo simulation code designed for a use with large atomic structures

Jagielski Jacek^{1,2,*}, Nowicki Lech¹, Mieszczyński Cyprian¹, Skrobas Kazimierz^{1,3}, Józwik Przemysław¹, Józwik Iwona^{1,2}, Thomé Lionel⁴, Garrido Frédéric⁴, Gentils Aurelie⁴

¹*National Centre for Nuclear Research, NOMATEN CoE MAB+ Division, A. Sołtana 7, 05-400 Otwock, Poland*

²*Łukasiewicz Institute for Microelectronic and Photonics, Wolczyńska 133, 01-926 Warszawa, Poland*

³*Institute of High Pressure Physics PAS, ul. Sokółowska 29/37, 01-142 Warsaw Poland*

⁴*Irene Joliot-Curie Lab, Bât. 100, 15 rue Georges Clémenceau, 91405 Orsay cedex, France*

A new tool for Monte Carlo simulation of ion channeling in crystals is described. The recently developed McChasy2 code follows the algorithm used previously in the McChasy program, but is well suited for simulations in large crystalline samples containing even several hundred millions of atoms. Main aim of the new version is to treat large crystalline cells created via Molecular Dynamics simulations, the cells may include complex defects such as dislocations, dislocation loops, stacking faults, layered structures etc. The code is able to reproduce channeling spectra from structural models, it may serve thus the purpose of development and validation of atomistic models of defect formation in crystals. The state of works on the validation of the code, and the possibilities of the new code for supplementing molecular dynamics with a tool supporting the experimental analysis of crystalline structures are presented. The code is currently used for the analysis of structures in irradiated metals, but it can be used in the studies of defects in any kind of crystalline materials.

Last part of the talk will be devoted to the presentation of the NOMATEN Teaming project and current trends in studies of materials for nuclear applications in Europe.

Ion-irradiated damage-induced resistivity contrast imaging of semiconductor structures with ultra-low energy electrons

Jóźwik I.^{1,2)}, Jagielski J.^{1,2)}, Dumiszewska E.¹⁾, Kamiński P.^{1,3)}, Caban P.¹⁾ and Kentsch U.⁴⁾

¹⁾*Lukasiewicz Research Network – Institute of Microelectronics and Photonics, Al. Lotników 32/46, Warsaw, Poland*

²⁾*National Centre for Nuclear Research, Department of Physics, 7th A. Soltana Str., Świerk-Otwock, Poland*

³⁾*Warsaw University of Technology, Institute of Microelectronics and Optoelectronics, Pl. Politechniki 1, 00-661 Warsaw, Poland,*

⁴⁾*Institute of Ion Beam Physics and Materials Research, Helmholtz-Zentrum Dresden-Rossendorf e.V. (HZDR), D-01328, Dresden, Germany*

The technique of implant isolation by ion irradiation with various energetic ions was found applicable in the microelectronic industry to create insulating regions in electronic semiconductor devices. To verify the extent of the modified area, usually the wet selective etching is used. However, it cannot be applied to materials, for which selective etchants do not exist (i.e. GaN). The low-voltage scanning electron microscopy (low-kV SEM) paves the way towards new applications in semiconductor technology to detect contrast originating from highly insulating channels produced by ion damaging of semiconductors.

The AlGaAs, GaAs, InAlP and GaN epitaxial layers grown by (MOCVD) technique were covered with the mask of gold stripes and irradiated with He⁺ ions of energy 600 keV with fluencies ranging from 8e12 to 5e14 cm⁻². The ion-irradiation damage effects in semiconductors in cross-sectional view after cleavage were directly visualized by means of scanning electron microscopy at low energy operation (E<0.5 keV) using high-resolution SEM SU8230 (Hitachi) and Auriga (Carl Zeiss), both equipped with the highly efficient in-lens SE detection systems.

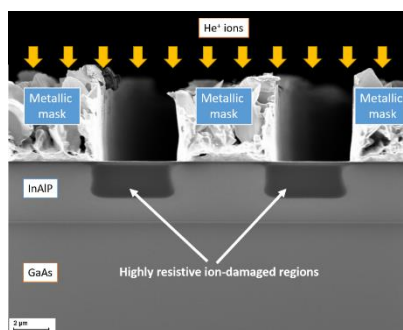


Figure 1: SEM image of InAlP layer cross-section with visible ion-damaged regions

Secondary electron images collected at low energy of primary electrons show strong contrast related to the local differences in the material resistivity resulting from the ion-

induced damage (Fig. 1). The SEM imaging with the Damage-Induced Voltage Alteration (DIVA) contrast [1-3] can serve as a tool to reveal qualitatively the information on the ion-irradiation damage level in semiconducting materials. without a need of complex sample preparation.

Acknowledgment

This work has been financed by the National Science Centre, Poland, under the grant number 2017/27/B/ST8/01158. I.J. acknowledge support by RADIATE project under the Grant Agreement 824096 from the EU Research and Innovation program HORIZON 2020.

References

- [1] Jóźwik I., Barcz A., Dąbrowska E., Dumiszewska E., Michałowski P.P., Ultramicroscopy 2019;204:6
- [2] Jóźwik I., Jagielski J., Dumiszewska E., Kamiński M., Kentsch U., Ultramicroscopy 2021;228:113333
- [3] Jóźwik I., Jagielski J., Caban P., Kamiński M., Kentsch U., Materials Science in Semiconductor Processing 2022;138:106293

Swift heavy ion modification of A_3B_5 nanoparticles and zinc- based core-shell nanostructures embedded in silica

Komarov F.¹⁾, Vlasukova L.²⁾, Makhavikou M.¹⁾, Parkhomenko I.²⁾, Yuvchenko V.¹⁾, Milchanin O.¹⁾, Dauletbekova A.³⁾, Žuk J.⁴⁾, Janse van Vuren F.⁵⁾, Neethling J.⁵⁾

¹⁾A.N.Sevchenko Institute of Applied Physics Problems, Kurchatov Str. 7, 220045 Minsk, Belarus

²⁾Belarusian State University, Independence Ave. 4, 220030 Minsk, Belarus

³⁾L.N.Gumilev Eurasian National University, Munaitpassov Str. 5, 010008, Nur-Sultan, Kazakhstan

⁴⁾Maria Curie-Skłodowska University, Pl. M. Curie-Skłodowskiej 1, 20-031 Lublin, Poland

⁵⁾Centre for HRTE, N.Mandela Metropolitan University, 6031, Port Elizabeth, South Africa

Swift heavy ion (SHI) irradiation is a promising technique to modify the properties of nanoparticles embedded in silica. It can act as a size filter for metal nanoparticles in silica by means of dissolution of small (less than 2 nm) precipitates and by narrowing of size distribution of bigger ones [1, 2]. It can also elongate nanoparticles embedded in insulating matrices (ion-shaping!). The elongation direction can be controlled by the SHI beam and all of the NPs are elongated in the same direction [3, 4].

The ion-shaping has been studied predominantly for metal nanoparticles embedded in silica due to their prominent plasmonics properties. Yet very little work has been done for nanoparticles of binary semiconductors. Ensembles of II-VI and III-V nanoparticles (NPs)/nanorods inside SiO_2 are of interest for applications in optoelectronics devices (light emitting diodes, photodetectors, lasers) operating in the UV, visible and IR range.

In this report we present the results of shape transformation and light-emitting properties of ion-beam synthesized InAs and Zn-based nanoparticles embedded in silicon dioxide films on silicon and afterwards irradiated with swift Xe ions (167 and 200 MeV, $2\text{--}3 \cdot 10^{14} \text{ cm}^{-2}$).

References

- [1] Ramjaun Y, et al, J. Appl. Phys. 2010; 10:104303.
- [2] Yang Y, et al, NIMB 2013; 308:24.
- [3] Komarov F, Physics-Uspekhi 2017; 60:435–471.
- [4] Ion-beam modification of solids, Springer, Ed. by W.Wesch, E.Wendler, 2016;534.

Europium implanted ZnO-based quantum structures

Kozanecki A.¹⁾, Sajkowski J.M.¹⁾, Mathew J.A.¹⁾, Zhydachevskyy Y.¹⁾, Alves E.²⁾ and Stachowicz M.¹⁾

¹⁾*Institute of Physics, PAS, Al. Lotnikow 32/46, 02-668 Warsaw, Poland*

²⁾*Univ Lisbon, Inst Plasmas & Fusao Nucl, P-2695066 Bobadela, Portugal*

In white light sources based on GaN, the blue and green colours are generated directly in the electroluminescence diodes, while the red colour is generated in external phosphors. Therefore, attempts are being made to obtain red light by doping light emitting diodes. Europium is an admixture that is intensively tested to obtain a red emission around 620 nm. As it is known, in order to obtain efficient emission of Eu^{3+} ions from GaN it is necessary to dope it with Mg and O. Therefore, in this work photoluminescence (PL) of Eu ions implanted into single layers of ZnO, ZnMgO and in short-period ZnO/ZnMgO and ZnO/MgO superlattices (SLs) is investigated. All the structures were grown by Molecular Beam Epitaxy on different substrate including sapphire, GaN/sapphire templates and crystalline ZnO. The samples were implanted with 300 keV Eu ions at 300°C. Then rapid thermal annealing was performed at 800°C, 5 minutes, in an oxygen atmosphere to activate the intra-4f-shell PL of Eu^{3+} ions. After annealing the red emission due to the $^5\text{D}_0 \rightarrow ^7\text{F}_2$ radiative transitions of Eu^{3+} was observed at excitation above the energy gap. The results show that the red emission is an order of magnitude more efficient in ZnMgO layers than in single ZnO layers. Similarly, the emission is intense in ZnO/ZnMgO superlattices. The results clearly show that Mg is essential for obtaining the high 4f-4f PL intensity of Eu^{3+} ions. The PL excitation spectra were studied to confirm the energy transfer from the band gap to the Eu^{3+} ions. A clear evidence is presented that in the studied short period SLs, the excitation of the Eu^{3+} PL occurs via generation of excitons in the barrier layers. We also present our first attempts to grow ZnO and ZnMgO layers doped with Eu during MBE growth. SIMS measurements confirm that doping during growth to the level of 10^{21} cm^{-3} was successful. The $^5\text{D}_0 \rightarrow ^7\text{F}_2$ radiative transitions of Eu^{3+} were observed in as-grown samples as well as in annealed at oxygen flow.

SHI induced bulk rotation in non-amorphizable targets

O'Connell J. and Douglas-Henry D.*

CHRTEM, Nelson Mandela University, South Africa

An interesting and relatively under studied effect of SHI irradiation at off normal incidence is that of induced rotation in materials. The effect was first observed in amorphous glasses and was explained via a continuum mechanics approach in [1]. Since then, rotation has been observed in several polycrystalline and single crystalline systems using mainly surface shifts and X-ray diffraction to measure rotation angle [2,3]. Without directly imaging the microstructure it was suspected that crystalline specimens would partially amorphize under irradiation and that grain rotation was facilitated by the amorphous matrix in which the remaining crystallites were suspended. Recent electron microscope-based analysis proved this assumption to be incorrect and instead it is believed that rotation is a consequence of complex dislocation motion due to off normal ion hammering stresses.

A case study of 593 MeV Au irradiated single crystal (001) oriented NiO will be presented as the simple NaCl structure limits the number of required slip systems when the irradiation geometry is suitably symmetric. In order to gain insight on the rotation mechanism, depth (and thus S_e) dependent rotation curves were extracted from electron backscatter diffraction maps of cross sectionally polished specimens and TEM was used to study the microstructure of irradiated specimens. Comparison of SEAD rotation vs depth profiles to those obtained through EBSD which do not require electron transparent lamellae shows that little to no relaxation occurs upon thinning indicating a mostly plastic deformation and relaxed microstructure.

References

- [1] S. Klaumünzer, *Nucl. Inst. Meth. B*, 215 (2004) 345-352
- [2] I. Zizak, N. Darowski, S. Klaumünzer, G. Schumacher, J. W. Gerlach, and W. Assmann, *Nucl. Inst. Meth. B*, 267 (2009) 944-948
- [3] I. Zizak, G. Schumacher, N. Darowski, and S. Klaumünzer, *Phys. Rev. Lett.*, 101 (2008) 1-4

* joconnell@mandela.ac.za

Negative ion formation by low energy electron interaction with molecules

Pelc Andrzej

Maria Curie-Skłodowska University, Institute of Physics, Department of Biophysics, Mass Spectrometry Laboratory, Pl. M. Curie-Skłodowskiej 1, 20-031 Lublin, Poland

In the case of electron – molecule interaction, the incoming electron may be trapped in the vicinity of the molecule forming an (excited) temporary negative ion (TNI). Electron attachment is a resonant process, i.e. the electron energy must match with an appropriate state of the TNI. Obviously, the energy of the TNI is higher than the ground state of the molecule and electron in the continuum state, so the temporary negative ion is unstable. Most probably, the energy excess in the TNI can be released by two processes, autodetachment or dissociative electron attachment (DEA). The autodetachment process causes the emission of the captured electron. In the DEA process, the TNI dissociates into a thermodynamically stable anion and a neutral fragment(s).

The electron attachment spectrometer used in the present studies comprises of a molecular beam source, a high resolution electron monochromator (EM) and a quadrupole mass filter (QMS) with a pulse counting system for analysing and detecting the ionic products. The vapour of studied compound was directly introduced into the interaction chamber of the EM by a capillary. The anions generated by the electron attachment process were extracted by a weak electrostatic field into the quadrupole mass spectrometer where they were analysed and detected by a channeltron secondary electron multiplier.

The several results regarding the negative ion formation will be presented and discussed.

Influence of noble gas ions irradiation on the structural and magnetic properties of HTS-2G tapes

Pęczkowski Paweł

Institute of Physical Sciences, Faculty of Mathematics and Natural Sciences. School of Exact Sciences, Cardinal Stefan Wyszyński University, K. Wóycickiego 1/3 Street, 01-938 Warsaw, Poland

In the presentation I will discuss the influence of noble gas ion irradiation on the critical parameters of HTS-2G SF 12050 high-temperature superconducting tapes based on GdBCO ($\text{GdBa}_2\text{Cu}_3\text{O}_{7-\delta}$ where δ is oxygen factor). Such tapes can be used to shield spacecraft and astronauts from radiation in space, where there are low temperatures. In outer space, tapes are exposed to various types of radiation, mainly protons, α (He atom) particles, but also ions of other elements, including noble gas elements such as Ne^+ , as well as Ar^+ , Xe^+ . Various types of defects appear in the tape during implantation, including Frenkel defects that serve as the fixation centers of Abrikosov vortices. These defects affect the superconducting and structural parameters of the irradiated tapes. In order to determine the influence of ions fluency on the parameters of superconductivity of GdBCO-based tapes with critical current densities (J_c) 3.7 MAcm^{-2} at liquid nitrogen temperature (77 K), width and length $5.0 \pm 0.1 \text{ mm}$ and thickness $50.0 \pm 0.1 \mu\text{m}$, the Ag protective layer of the tape was removed by a catalytic process. Next, the noble gas Ne^+ ions with an energy of 250 keV and four different fluences were implanted: 10^{12} , $5 \cdot 10^{12}$, 10^{13} , and $10^{14} \text{ Ne}^+/\text{cm}^2$. The SF 12050 tapes were prepared to obtain a homogeneous implantation surface on the sample surface. Microstructural (SEM - scanning electron microscopy with EDS - energy dispersive spectroscopy) and structural (XRD - X-ray diffraction) tests were carried out. The c lattice parameter decreases with longer irradiation times, which may be associated with a decrease in the oxygen index. decrease in J_c for irradiated versus non-irradiated samples and a slight decrease in critical temperature (T_c) of 1.5 – 2.0 K for irradiated tapes (T_c for non-irradiated 93.5 K tape).

Defect engineering in degenerate semiconductors using intense pulsed light

Prucnal Sławomir^{1,2)}

¹⁾*Helmholtz-Zentrum Dresden-Rossendorf, Institute of Ion Beam Physics and Materials Research, Bautzner Landstrasse 400, 01328 Dresden, Germany*

²⁾*Maria Curie-Skłodowska University, Pl. M. Curie-Skłodowskiej 1, 20-031 Lublin, Poland*

The n-type doping of Ge is a self-limiting process due to the formation of vacancy-donor complexes (D_n-V with $n \leq 4$) that deactivates the donors. Based on data density functional theory calculations, at temperature higher than 850 K, the concentration of D_4-V clusters progressively decreases liberating unbounded vacancies and donor atoms. Next the free monovacancies are trapped by big vacancy clusters causing high activation efficiency of donors in Ge. Similar problems apply to III-V compound semiconductors, where, e.g. in GaN the p-type doping is challenging, or highly n-type layer formation in GaAs. That is mainly due to the high activation energy for acceptors, low equilibrium solid solubility and deactivation of dopants by the formation of dopant-vacancy clusters. Here, we report on experiments and theoretical calculations solving the basic problem of donors and acceptors deactivation in heavily doped semiconductors. The dissolution of donor/acceptor-vacancy clusters in heavily doped semiconductors is achieved by ms-range FLA with a peak temperature close to the melting point of the semiconductor. Positron annihilation lifetime spectroscopy (PALS) reveals that dopant-vacancy clusters are the main defect centers deactivating both acceptors and donors. Millisecond-range high-temperature treatment dissociates the dopant-V clusters and, as shown by SIMS, fully suppresses the dopant diffusion in both group IV semiconductors and III-V compound semiconductors. For the first time, using structural characterization (PALS, SIMS) and electrochemical capacitance-voltage profiling combined with DFT calculations, we were able to address, understand, and solve the fundamental problem hindering the doping of semiconductors above the solid solubility limit.

This work was partially supported by the German Academic Exchange Service (DAAD, Project-ID:57216326) and National Science Centre, Poland, under Grant No. 2016/23/B/ST7/03451.

Comprehensive approach to the studies of Zinc Oxide implanted with rare-earth ions for future optoelectronic device applications

Ratajczak Renata¹⁾, Guzewicz Elżbieta²⁾, Prucnal Sławomir³⁾, Mieszczynski Cyprian¹⁾, Jozwik Przemysław¹⁾, Turos Andrzej^{1,4)}, Krajewski Tomasz A.²⁾, Wozniak Wojciech²⁾, Wierzbicka Aleksandra²⁾, Heller Rene³⁾, Kentsch Ulrich³⁾, Facsko Stefan³⁾

¹⁾National Centre for Nuclear Research, Otwock, Poland

²⁾Institute of Physics, Polish Academy of Sciences, Warsaw, Poland

³⁾Helmholtz-Zentrum Dresden-Rossendorf, Dresden, Germany

⁴⁾Lukasiewicz Research Network - Institute of Microelectronics and Photonics, Warsaw, Poland

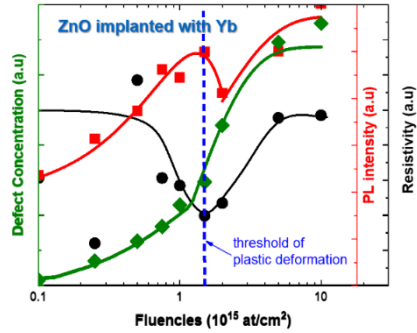
Nowadays, material research is driven by the search for new technologies that aim to improve existing materials and replace them with cheaper and more efficient equivalents. Since several decades, the semiconductor compounds technology has been perfectly in line with this trend. New technologies are essential for optoelectronic applications such as lasers, displays, or white LEDs, where silicon cannot be used due to its indirect and moderate bandgap.

Zinc Oxide (ZnO) is a transparent conductive material with a wide and direct bandgap (~ 3.37 eV), similar to that of GaN. However, the technology of growing ZnO crystals and layers is much easier and cheaper than the technology of GaN production. Especially attractive is the growth of ZnO films by the Atomic Layer Deposition (ALD) method, which is perspective for large-scale industrial applications and also fulfills very well the requirements of organic electronics. The basic light emission from ZnO is located in the UV spectral range, but it can be tuned into the visible region by rare-earth (RE) ions doping.

In this work, the results of structural, optical, and electrical studies will be presented for ZnO doped with RE by ion implantation. Although implantation is a convenient method for RE doping, an important limitation of this technique is the structure defects buildup, which might result in luminescence quenching. Annealing, which is carried out to crystal lattice recovery, in turn, leads to defect interactions, clustering, and many other adverse phenomena.

Our studies, performed on epitaxial ZnO-ALD films implanted with several RE ions, show that the post-implantation defect accumulation process does not depend of the type of RE ion used. In contrast, the level of lattice structure recovery and the RE-ions behavior after annealing are no longer the same, strongly influencing the color of the emitted light. Moreover, we have found that the optical and electrical properties are strongly connected with the threshold of structural transformation, which is evidenced by the fact that above the threshold of plastic deformation, the luminescence quenching and resistivity decreasing effects take place.

I will show you also our successes and failures as well as reasonable compromises that we made trying to obtain white light source emitters based on this material. The defect interactions and clustering during RE implantation and subsequent annealing, make the problem of effective light emission quite complex and require a variety of complementary analytical



*R. Ratajczak et al.
Appl. Surf. Sci. 521 (2020) 146421*

methods. For example, RBS/c and HRXRD data provide different aspects of defect accumulation. In turn, the study of electrical properties of ZnO:RE interestingly complements the luminescence data as it provides information about ionization, which is strongly related to the optical response of the system. The important milestone to achieve this goal was also the development of a method for quantitative analysis of extended defects by Monte Carlo simulation. The obtained information allows for deciding on the number, location, and configuration of the RE-induced defects ('defects engineering').

Acknowledgment

This research was carried out under the co-financed international project supported by the Polish Ministry of Education and Science (3846/HZDR/2018/0 and 5134/HZDR/2020/0) and Helmholtz-Zentrum Dresden-Rossendorf (17000941-ST, 20001987-ST).

Surface modification of zirconium alloys used for claddings to improve the corrosion resistance

Sartowska B.¹⁾, Barlak M.²⁾, Starosta W.¹⁾, Waliś L.¹⁾, Smolik J.³⁾

¹⁾*Institute of Nuclear Chemistry and Technology, Dorodna 16, 03-195 Warsaw, Poland*

²⁾*National Centre for Nuclear Research, A. Sołtana 7, 05-400 Otwock, Poland*

³⁾*Łukasiewicz Research Network - The Institute for Sustainable Technologies, K. Pułaskiego 6/10, 26-600 Radom, Poland*

Zirconium alloys are commonly used as cladding material for fuel elements in nuclear reactors. This application is connected with zirconium alloys good water corrosion and radiation resistance at normal working conditions of nuclear reactor. In the case of severe accident conditions, the possible very fast zirconium alloys oxidation at steam or/and air atmosphere may result in intense hydrogen generation and hydrogen-oxide mixture explosion. Advanced materials that are intended to be more tolerant of severe accident conditions with the safe operation under normal conditions are looking for. One of concept is to improve corrosion resistance of Zr alloys cladding with surface modification or/and protective coatings formation.

The aim of presented study was to develop, form and investigate coatings on zirconium alloys. Experiments with (i) Cr, Y, Al incorporation using intense pulsed plasma beams, (ii) surface layer electron beam remelting, (iv) multielemental Zr-Si-Cr coatings formation using PVD method were carried out. Heat treatment in argon, air oxidation and corrosion tests in standard conditions for PWR reactors (360oC/195 bar/water simulating water used in PWR) were carried out. Initial, modified and tested materials were characterized with SEM (morphology observations), EDS (elemental composition determination), XRD (phase composition analysis).

Obtained results showed protective character of formed layers in defined experiments parameters range.

ORAL PRESENTATIONS

Microstructural response of silicon nitride to fission fragments

Janse van Vuuren Arno¹⁾, Ibrayeva Anel¹⁾, Skuratov Vladimir²⁾, Zdorovets Maxim³⁾

¹⁾*Centre for HRTEM, Nelson Mandela University, Port Elizabeth, South Africa*

²⁾*Flerov Laboratory for Nuclear Research, Joint Institute for Nuclear Research, Dubna, Russia*

³⁾*Institute of Nuclear Physics, Astana, Kazakhstan*

Si₃N₄ is not only an important semiconductor material but is also under consideration for use as candidate-inert-matrix-fuel-hosts (IMs) for the burn-up of plutonium and minor actinides [1,2]. IMs are envisioned as one possible means to close the nuclear fuel cycle in an effort to reduce the amount of high-level waste materials which require long-term storage [3]. The physical properties of this material make it well suited to reactor conditions [2]. However, to prove the viability for nuclear applications its' radiation stability must be tested. In this investigation swift heavy ions are therefore used to simulate the effects of fission fragments on microstructure of Si₃N₄.

To assess the behaviour of different phases of Si₃N₄ under irradiation, polycrystalline (Al doped) bulk samples, amorphous thin films and nanoparticles were irradiated with ions of varying stopping power. The samples were irradiated with Xe (167, 220, 480 MeV) and 710 MeV Bi ions. Selected samples were also irradiated with 220 MeV Xe ions at temperatures ranging from LNT to 1000 K. The microstructural effects of swift heavy ions on these materials were analysed using transmission electron microscopy techniques. The effect of fission fragments on the microstructure of Si₃N₄, through electronic energy deposition processes, and the formation of latent tracks in crystalline (including nanocrystalline), amorphous and radiation-induced-amorphous phases of silicon nitride will be presented.

References

- [1] Yamane, J. et al. (2008) Progress in Nuclear Energy 50, 621.
- [2] Nappé, J.C. et al. (2011) Nucl. Instr. and Meth. in Phys. Res. B 269, 100.
- [3] Lee, Y.-W. et al. (2001) Metals and Materials 7(2), 159.

Optical spectra and chemical composition of native oxide layers on hot-implanted GaAs

Kulik M.^{1,2)}, Kołodynska D.³⁾, Żuk J.¹⁾, Hubicki Z.³⁾ and Turek M.¹⁾

¹⁾*Institute of Physics, Maria Curie-Skłodowska University, Lublin, Poland*

²⁾*The Frank Laboratory of Neutron Physics JINR, Dubna Russia*

³⁾*Faculty of Chemistry, Maria Curie-Skłodowska University, Lublin Poland*

Oxygen atoms from air create dielectric layers of native oxides on semiconductor surface in normal conditions. The surfaces of (100) semi-insulating (SI) GaAs samples are irradiated with 200 keV Al⁺ ions at room temperature (RT) and temperatures: 250, 300, 350, 400, 450 and 500°C, and the accumulated fluence on each sample was $3 \times 10^{16} \text{cm}^{-2}$. This process was used to form box-like Al atomic depth profiles in the studied samples, subsequently investigated by the secondary ion mass spectrometry (SIMS). It was observed that the concentration of Al atoms increases near the surface of the implanted samples.

In the studies of hot-implanted GaAs performed by the spectroscopic ellipsometry (SE) method a local maximum is observed in the UV region of the optical spectra, which is absent in the spectrum of non-implanted GaAs. The peak's height varies with the temperature of the samples during ion implantation.

Nuclear Reaction and Rutherford backscattering spectrometry (NR/RBS) investigations on hot-implanted GaAs showed the thickness values of the native oxide layers between 5 and 10 nm.

In the next step, X-ray photoelectron spectroscopy (XPS) method was used to study chemical composition of the native oxide layers formed on the samples in the air after the implantation process. It was found that the following compounds: Ga₂O₃, As₂O₃, As₂O₅, GaAs and Al₂O₃ are present in the oxide layers after the implantation. It was observed that the concentration of As₂O₅ decreases and that of GaAs and Al₂O₃ slowly grows when the temperature of the implantation samples increases. The results of the reported study using all the methods presented above may suggest that during the Al⁺ ion implantation process of GaAs at elevated target temperatures the Al diffusion process takes place towards the ion-irradiated surface with local formation of AlGaAs alloy.

Effect of nitrogen ion implantation on cavitation erosion resistance of CoCrWC alloy

Szala M.^{1)*}, Chocyk D.²⁾, Turek M.³⁾, Skic A.⁴⁾

¹⁾Department of Materials Engineering, Faculty of Mechanical Engineering, Lublin University of Technology, Nadbystrzycka 36D, 20-618 Lublin, Poland

²⁾Department of Applied Physics, Faculty of Mechanical Engineering, Lublin University of Technology, Nadbystrzycka 36D, 20-618 Lublin, Poland

³⁾Institute of Physics, Maria Curie-Skłodowska University in Lublin, pl. M. Curie-Skłodowskiej 1, 20-031 Lublin, Poland

⁴⁾Department of Mechanical Engineering and Automatic Control, University of Life Sciences, Głęboka 28, 20-612 Lublin, Poland

The work investigates the effect of nitrogen ion implantation (NII) of HIPed Stellite 6 (CoCrWC alloy) on the improvement of resistance to CE. The CE resistance of stellites ion-implanted by 120 keV N⁺ ions at two fluences: $5 \times 10^{16} \text{ cm}^{-2}$ and $1 \times 10^{17} \text{ cm}^{-2}$ were comparatively analysed with the unimplanted stellite and AISI 304 stainless steel. CE tests were conducted according to ASTM G32 with stationary specimen method. Erosion rate curves and mean depth of erosion confirm that the nitrogen-implanted HIPed Stellite 6 two times exceeds the resistance to CE than unimplanted stellite, and has almost ten times higher CE reference than stainless steel. The X-ray diffraction (XRD) confirms that NII of HIPed Stellite 6 favours transformation of the $\epsilon(\text{hcp})$ to $\gamma(\text{fcc})$ structure. Unimplanted stellite ϵ -rich matrix is less prone to plastic deformation than γ and consequently, increase of γ phase effectively holds carbides in cobalt matrix and prevents Cr₇C₃ debonding. This phenomenon elongates three times the CE incubation stage, slows erosion rate and mitigates the material loss. Metastable γ structure formed by ion implantation consumes the cavitation load for work-hardening and $\gamma \rightarrow \epsilon$ martensitic transformation. In further CE stages, phases transform as for unimplanted alloy namely, the cavitation-induced recovery process, removal of strain, dislocations resulting in increase of γ phase.

* email: m.szala@pollub.pl

Modification of PET foil properties by 150 keV Li⁺ ion implantation

Turek M.¹⁾, Drożdżiel A.¹⁾, Pysznia K.¹⁾, Grudziński W.¹⁾, Węgierek P.²⁾

¹⁾Maria Curie-Skłodowska University, Pl. M. Curie-Skłodowskiej 1, 20-031 Lublin, Poland

²⁾Lublin University of Technology ul. Nadbystrzycka 38 D, 20-618 Lublin

In the paper the influence of 150 keV Li⁺ ion irradiation (with fluences in the range from 10¹⁴ cm⁻² up to 2·10¹⁶ cm⁻².) on microstructural, optical and electrical properties of very thin PET foils is studied. Raman and UV-VIS spectroscopy measurements confirmed destruction of numerous bonds within the polymer intensifying with the irradiation fluence. Changes in the Raman spectra, namely the presence of broad D and G band being the fingerprint of amorphous graphitelike structures, point out at formation of carbon clusters made of sp² hybridised C atoms. The fact that the D band is much less pronounced than the G one suggests that the graphitelike structures are built rather of carbon rings than chains, unlike in the previously considered case of Na⁺ or K⁺ implantation. The evolution of absorbance spectra also could be understood as a consequence of formation of carbon clusters and a formation of conducting structures in the modified layer. The reduction of the optical bandgap from its initial value (3.95 eV) down to 1.4 eV for the most heavily treated sample is observed, but this effect is not as strong as in the case of heavier projectiles like K⁺ or Na⁺ (close to 0.5 eV). The average size of carbon clusters is also smaller – reaching several hundreds of C atoms. The ion irradiation introduces disorder to the polymer and results in the emergence of additional energy levels within the bandgap. Urbach energy increases from 55 meV to ~ 1.2 eV in the case of the sample implanted with fluence 2·10¹⁶ cm⁻². The changes in the microstructure lead to the reduction of electrical sheet resistivity of the modified samples by e.g. 2.5 orders of magnitude in the case of most heavily modified samples. The reduction of the resistivity is observed also on the non-implanted side of the foil.

References

[1] Turek M., Drożdżiel A *et al.* Acta Physica Polonica A 2019;136:278

Multicomponent dilute ferromagnetic semiconductors on the base of (Ga,Mn)As for spintronic applications

Yastrubchak O.¹⁾, Tataryn N.¹⁾, Wosinski T.²⁾, Sadowski J.^{2,3)}, Domagala J.Z.²⁾, Sawicki M.²⁾, Gluba L.⁴⁾ and Žuk J.⁴⁾

¹⁾*V.E. Lashkaryov Institute of Semiconductor Physics, NASU, U-03028 Kyiv, Ukraine*

²⁾*Institute of Physics, Polish Academy of Sciences, PL-02-668 Warszawa, Poland*

³⁾*Dept. Physics and Electrical Engineering, Linnaeus University, SE-391 82 Kalmar, Sweden*

⁴⁾*Institute of Physics, Maria Curie-Skłodowska University, PL-20-031 Lublin, Poland*

Dilute ferromagnetic semiconductors (DFSs) represent a class of alloys which combine semiconductor properties with magnetism in a single material. Their magnetic properties arise from transition metal ions introduced into the semiconductor parent lattice. Their magnetism can be tuned and manipulated by the electronic doping, strain, temperature, electrical gating, interband transitions, and other effects arising from applied electric field or optical illumination. This combination of electronic and magnetic properties results in entirely new physical properties that are of interest in basic science and, importantly, hold promise of a wide range of device applications referred to as spintronics. The unique property of DFS spintronic devices is their capability of generating spin-polarized currents. In addition to the formation of spin current, of interest to spintronics, it is expected that the band structure changes arising from the presence of different doping ions such as In or Bi in the (Ga,Mn)As matrix, will lead to further developing of novel DFS device concepts.

Our present research has confirmed that homogenous layers with high structural perfection of quaternary (Ga,Mn)(Bi,As), (In,Ga,Mn)As, and pentanary (In,Ga,Mn)(Bi,As) DFSs can be grown by low-temperature molecular beam epitaxy (MBE) and using ion implantation technique. Structural properties of the epitaxial layers have been studied using high resolution X-ray diffractometry (HRXRD). Due to the Mn-induced increase of the lattice constant the (Ga,Mn)As ternary alloy grown pseudomorphically on GaAs substrate suffers a biaxial compressive epitaxial strain, which influences its magnetic properties (magnetic anisotropy). The magnetic properties of the epitaxial layers have been analyzed with the superconducting quantum interference device (SQUID) magnetometry. Quaternary (Ga,Mn)(Bi,As), (In,Ga,Mn)As and pentanary (In,Ga,Mn)(Bi,As) layers can be obtained as strain-free DFS layers by growing them on the lattice matched (In,Ga)As buffer layer. Additionally, an easy tuning between tensile and compressive epitaxial strain can be achieved by appropriate selection of the In and Bi content that makes these alloys interesting for prototypical spintronic devices requiring fine tuning their magnetic anisotropy. These multicomponent alloys combine the properties of (Ga,Mn)As (ferromagnetism with the relatively high Curie temperature), Ga(Bi,As) (band structure modification) and (In,Ga)As (local strain creation). The incorporation of a small amount of Bi into (Ga,Mn)As layers results in a significant increase in the magnitude of their magneto-transport effects resulting from the enhanced spin-orbit interaction in the valence band.

Strongly increased separation of the spin-split-off hole band in both the Bi- and In-contained DFS layers has been confirmed by investigation of their valence band structure using the angle-resolved photoemission spectroscopy (ARPES) and modulation photoreflectance spectroscopy methods. The combination of those properties leads to a new family of materials that will help to first understand and later tailor their application-relevant properties. In particular, the deeper investigation of multicomponent alloy magnetic semiconductors will broaden the possibility of their bandgap engineering.

YOUNG SCIENTISTS CONTEST
ORAL PRESENTATIONS
POSTER PRESENTATIONS

Tolerance of nanocrystalline $\text{Y}_4\text{Al}_2\text{O}_9$ for SHI irradiation

*Ibrayeva A.^{1,2)}, O'Connell J.¹⁾, Mutali A.^{2,3,4)}, Korneeva E.³⁾, Sohatsky A.³⁾
and Skuratov V.^{3,5,6)}*

¹⁾Centre for HRTEM, Nelson Mandela University, Port Elizabeth, South Africa

²⁾Institute of Nuclear Physics, Almaty, Kazakhstan

³⁾Flerov Laboratory of Nuclear Reactions, JINR, Dubna, Russia

⁴⁾L.N. Gumilyov Eurasian National University, Nur-Sultan, Kazakhstan

⁵⁾National Research Nuclear University MEPhI, Moscow, Russia

⁶⁾Dubna State University, Dubna, Russia

Radiation tolerance of nanocrystalline $\text{Y}_4\text{Al}_2\text{O}_9$ (nc-YAM), being a key component of oxide dispersion strengthened ferritic alloys, is a popular research topic in recent times [1]. In this work structural changes induced by swift heavy ions (SHI) in a range of electronic stopping powers 6-35 keV/nm by means of high-resolution TEM are discussed. Bi and Xe ions were found to form continuous amorphous tracks in isolated nanocrystals (Fig.1) in contrast to this material's extremely high radiation stability in a metallic matrix [2]. Our work contributes new data towards a more comprehensive understanding of threshold conditions to ion track formation in nc-YAM.

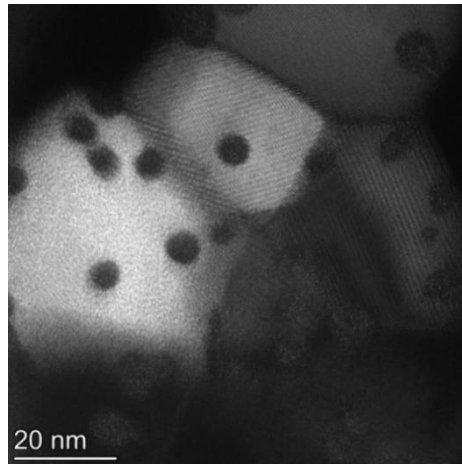


Fig. 1. DF TEM image of nc-YAM irradiated with Xe with energy of 0.2 MeV/u

Acknowledgement. This research was funded by the Ministry of Education and Science of the Republic of Kazakhstan (Grant No AP09058081).

References

- [1] Ukai S. et al. Struc. Mat. Gen.-IV Nucl. Reac. (2017), 357-414.
- [2] Rogozhkin S.V. et.al, Nucl. Instrum. Meth. Phys. Res. B 486 (2021), 1-10.

Ultra-high pressure doping of GaN with europium

Jaroszyński P.¹⁾, Grzanka E.¹⁾, Grabowski M.¹⁾, Jakiela R.²⁾, Sierakowski K.¹⁾, Prozheev I.³⁾, Tuomisto F.³⁾, Boćkowski M.¹⁾

¹⁾*Institute of High Pressure Physics PAS, Warsaw, Poland*

²⁾*Institute of Physics PAS, Warsaw, Poland*

³⁾*Department of Physics, University of Helsinki, Helsinki, Finland*

Europium doping of GaN is a promising method for the fabrication of optoelectronic devices capable of emitting red light efficiently [1], which constitutes a longstanding problem of display technology based on GaN. The traditional approach of chemical doping is problematic for Eu on account of rapid oxidation in ambient conditions and reactor poisoning effect. The research performed in this work presents the feasibility of an alternative doping method using the diffusion of ion implanted Eu into the volume of an ammonothermal GaN substrate annealed in ultra-high pressure conditions. The determined diffusion coefficients for Eu are 1.05×10^{-13} cm²/s and 344 meV for temperature independent diffusion coefficient (D_0) and activation energy (E_a), respectively. In addition to structural and morphological quality, photoluminescence originating from point defect complexes containing Eu is identified and discussed.

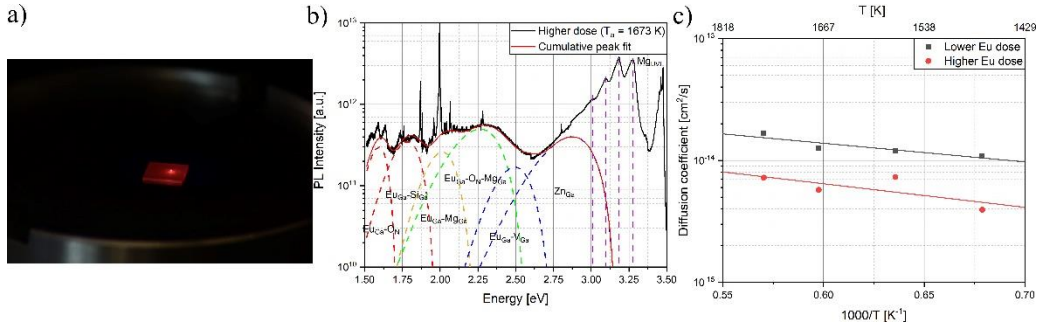


Figure 1: a) Room temperature PL of annealed GaN:Eu (1473 K), b) Arrhenius plot for $D(T)$, c) Identified PL bands originating from point defect complexes containing Eu.

References

- [1] Fujiwara Y, Ichikawa S, Timmerman D, Tatebayashi J, Proceedings Volume 11686, Gallium Nitride Materials and Devices XVI; 1168615 (2021) <https://doi.org/10.1117/12.2577199>

Modeling of dislocations and dislocation loops for Monte Carlo simulations of ion channeling

Józwik P.¹⁾, Mieszczynski C.¹⁾, Skrobas K.^{1,2)}, Ratajczak R.¹⁾, Jagielski J.^{1,3)}, Garrido F.⁴⁾, Alves E.⁵⁾, Lorenz K.^{5,6)}

¹⁾National Centre for Nuclear Research, Soltana 7, 05-400 Otwock, Poland

²⁾Institute of High-Pressure Physics PAS, Sokolowska 29/37, 01-142 Warsaw Poland

³⁾Lukasiewicz Institute of Microelectronics and Photonics, Wolczynska 133, 01-926 Warsaw, Poland

⁴⁾IJCLab, Université Paris-Saclay-CNRS, 91405 Orsay Campus

⁵⁾IPFN, Instituto Superior Técnico-Campus Tecnológico e Nuclear, Universidade de Lisboa, Estrada Nacional 10, 2695-066 Bobadela, Portugal

⁶⁾Instituto de Engenharia de Sistemas e Computadores - Microsistemas e Nanotecnologias, Rua Alves Redol 9, 1000-029 Lisbon, Portugal

Ion channeling is a common technique to study post-implantation damage in single crystals. However, measured energy spectra contain combined signals coming from different kinds of defects, which separation is hardly possible without the use of computational methods, e.g., Monte Carlo simulations. One of the codes used to achieve this goal is called McChasy-1.0. The software is capable to fit the experimental channeling spectra by simulating trajectories of light ions ($^4\text{He}^+$, $^1\text{H}^+$, $^2\text{H}^+$) in small structures (up to $\sim 10^2$ at.) in the presence of defects. The structures are deformed during ongoing simulations, based on defect models applied in the code and given depth-distributions of defects. Recent achievements of the McChasy-1.0 code are models of extended defects: dislocations and dislocation loops.

The model of dislocations requires some geometrical parameters of dislocations for a given structure, as it assumes that atomic planes adjacent to an extra half-plane of dislocation are bent following the arctan function (Peierls-Nabarro approach). To date, coefficients of the function have been determined using high-resolution Transmission Electron Microscopy (HRTEM) for several structures only (AlGaN, SrTiO₃, and ZnO) [1]. Here we report the current state of the McChasy-1.0 code and explain the principle of the simulation procedure in the presence of point and extended defects. Moreover, having in mind that the HRTEM analysis is expensive and destructive for samples, we discuss another way to determine the parameters of dislocations, which is based on Molecular Dynamics (the LAMMPS code). We describe the modeling of edge dislocations and dislocation loops in structures of Ni (a promising material for a new generation of nuclear power plants) and ZnO (a powerful semiconductor for electronic and optical applications). The coefficients of the arctan function found this way were used in the McChasy-1.0 code to fit selected channeling spectra and obtained defect profiles are presented as a result.

References

- [1] P. Jozwik, L. Nowicki, R. Ratajczak, C. Mieszczynski, A. Stonert, A. Turowski, K. Lorenz, and E. Alves, Advanced Monte Carlo Simulations for Ion-Channeling Studies of Complex Defects in Crystals. in Theory and Simulation in Physics for Materials Applications: Cutting-Edge Techniques in Theoretical and Computational Materials Science (eds. Levchenko, E. V., Dappe, Y. J. & Ori, G.) 133–160 (Springer International Publishing, 2020). doi:10.1007/978-3-030-37790-8_8.

Radiation resistance studies of PIN diode detectors irradiated with heavy ions

Krutul K.Z.¹⁾, Horodek P.²⁾, Napiorkowski P.J.¹⁾, Hadyńska-Klęk K.¹⁾, Komorowska M.¹⁾, Olejniczak A.³⁾, Paluch-Ferszt M.¹⁾, Siemek K.²⁾, Szepliński Z.¹⁾, Wróbel M.⁴⁾, Wrzosek-Lipska K.¹⁾

¹⁾Heavy Ion Laboratory, University of Warsaw, Pasteura 5A, 02-093 Warsaw, Poland

²⁾Institute of Nuclear Physics, Polish Academy of Sciences, Walerego Eljasza Radzikowskiego 152, 31-342 Kraków, Poland

³⁾Nicolaus Copernicus University, Jurija Gagarina 11, 87-100 Toruń, Poland

⁴⁾Faculty of Metals Engineering and Industrial Computer Science, AGH University of Science and Technology, Krakow, Poland

The exposition of semiconductor detectors to the ionizing radiation leads to their faster wear or damage. In particular, the radiation resistance of PIN diodes used in various measuring systems is a topical problem despite intense studies. The tests of the such detectors response to the high flux of gamma quanta [1], neutrons [2], protons and electrons [3] are reported in the literature. In practice, the quality of the energy spectrum of the registered particles becomes worse over the time. The reason of phenomenon can be found in the irradiation-induced changes in the structure of PIN diodes. The results of experimental studies focused on radiation damage process of the 300 μm PIN diode type detectors are going to be shown. PIN diodes were irradiated with two ion beams: ^{12}C with energy 45 MeV and ^{14}N with energy 35 MeV. The spectroscopic properties of these detectors were monitored by measuring the spectrum collected off-beam with the ^{241}Am α source. In turn, positron lifetime investigations delivered information about the irradiation-induced defects introduced by ions. The optical microscopy and optical profilometry completed the studies.

References

- [1] Abi B., Rizatdinova F., Proceedings of the Topical Workshop on Electronics for Particle Physics, 390-393 (2009).
- [2] Sopko V. et al. JINST, 8, C03014 (2013).
- [3] Johnston A. H., 4th International Workshop on Radiation Effects on Semiconductor Devices for Space Application, Tsukuba, Japan, October 11-13, 1-9 (2000).

Physical aspect of initiation and development of discharges in vacuum interrupters used in electric power switchgear

Lech M.¹⁾, Węgierek P.¹⁾ and Turek M.²⁾

¹⁾Lublin University of Technology, ul. Nadbystrzycka 38A, 20-618 Lublin, Poland

²⁾Maria Curie-Skłodowska University, Pl. M. Curie-Skłodowskiej 1, 20-031 Lublin, Poland

As part of the research work, the electrical strength of the contact system was measured for air and three noble gases: argon, helium, and neon, for contact gap equal to 1 mm and 2 mm. The characteristics of the electrical strength as a function of pressure for each of the gases are shown in Figure 1.

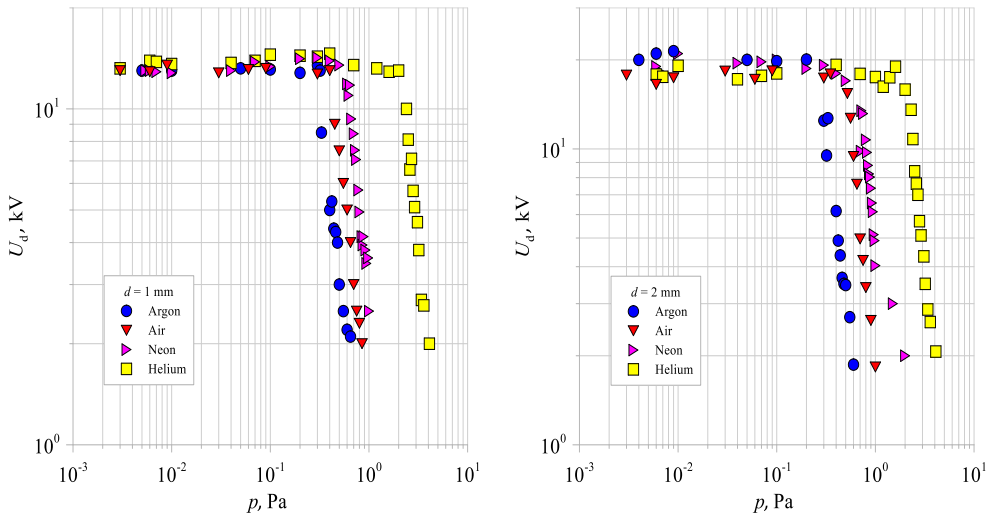


Figure 1: Dependence of breakdown voltage as a function of pressure, for contact gap $d = 1$ mm and $d = 2$ mm.

The obtained results of measurements of electrical strength of the contact system in the environment of air and three noble gases create promising possibilities for the production of new vacuum interrupters dedicated to modern medium-voltage switchgear. If neon or helium is used, it is possible to increase the rated operating pressure of such a vacuum interrupter, while retaining full insulating capability.

References

- [1] Opydo W.: Właściwości gazowych i próżniowych wysokonapięciowych układów izolacyjnych. Wydawnictwo Politechniki Poznańskiej, Poznań, 2008.

Modification of two-dimensional materials using ion implantation

*Li Yi^{1,2)}, Steuer Oliver¹⁾, Lin Kaiman^{1,2)}, Helm Manfred^{1,2)}, Zhou Shengqiang¹⁾
and Prucnal Slawomir¹⁾*

¹⁾*Institute of Ion Beam Physics and Materials Research, Helmholtz-Zentrum Dresden-Rossendorf, P.O.
Box 510119, 01314 Dresden, Germany*

²⁾*Technische Universität Dresden, 01062 Dresden, Germany*

The optimum solution for future nano-(opto-)electronics is the integration of direct band gap semiconductors with current Complementary Metal-Oxide-Semiconductor (CMOS) technology. 2D semiconductors are amongst the most promising future semiconductors. Single layer transition metal dichalcogenides (TMDCs) with the general formula MX_2 , where $\text{M} = \text{e.g. W or Mo}$ and $\text{X} = \text{S, Se, or Te}$ are characterized by direct bandgaps and high carrier mobilities. To realize low-power and high-performance electronic/optoelectronic devices based on 2D semiconducting TMDCs materials, several key parameters, such as contact resistance (RC), channel/contact doping (n- or p-type), and charge carrier mobility (for both electrons and holes), need to be effectively engineered to harness the maximum intrinsic efficiency in the device. Up to now, three basic intentional doping strategies have been tested: (i) in situ doping by substituting anions or cations during the growth, (ii) surface modification via intercalation, and (iii) electrostatic doping by gating. But those techniques does not provide stable and controllable doping that can be easily integrated with CMOS technology. Recently, we showed that efficient doping of a few layer thick MoSe_2 can be realized using Cl^+ ion implantation followed by sub-second annealing [1]. The successful doping of MoSe_2 was confirmed by I-V measurements and the red shift of the A_{1g} mode with increasing Cl concentration, which is due to the Fano interference caused by the coupling between discrete optical phonons and charge carriers.

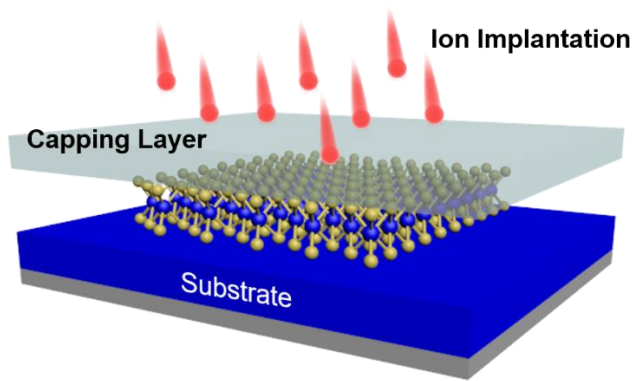


Figure 1 The ion implantation of two-dimensional materials using capping layers

Here, we extended our approach to the p-type and n-type doping in different TMDCs monolayer. MoSe_2 and WSe_2 monolayer, WS_2 monolayers are implanted through the

energy filter with P or Cl ions to form p-type and n-type layers, respectively. Both the micro-Raman and PL spectroscopies shows that the monolayers of TMDCs can survive the implantation process and implanted elements are stopped within the layer. The successful ion doping will allow us to fabricate lateral homojunctions, which is a milestone for the integration of TMDCs with CMOS technology and the production of devices with diverse functionalities.

References

- [1] S. Prucnal, A. Hashemi, M. Ghorbani-Asl, R. Hübner, J. Duan, Y. Wei, D. Sharma, D. R. T. Zahn, R. Ziegenrucker, U. Kentsch, A. V. Krasheninnikov, M. Helm, S. Zhou, *Nanoscale* 2021, 13, 5834.

Crystal lattice damage and recovery of rare-earth implanted wide bandgap oxides

Sarwar Mahwish¹⁾, Ratajczak Renata²⁾, Ivanov Vitalii¹⁾, Mishra Sushma¹⁾,
Turek Marcin³⁾, Guziewicz Elzbieta¹⁾

¹⁾*Institute of Physics, Polish Academy of Sciences, Al. Lotnikow 32/46, 02-668 Warsaw, Poland*

²⁾*National Centre for Nuclear Research, Soltana 7, 05-400 Otwock, Poland*

³⁾*Institute of Physics, Maria Curie-Skłodowska Univ., Pl. Skłodowskiej 1, 20-031 Lublin, Poland*

Rare earth (RE) materials are important for the optical tuning of wide bandgap oxides (WBO) as Ga_2O_3 or ZnO because they show narrow emission lines in the visible, ultra-violet and infra-red region. Ion implantation is an attractive method to introduce RE into the crystal lattice with extraordinary control of composition and location but it creates the lattice damage, which may cause RE to be optically inactive. Post-implantation thermal treatment of the implanted material at the appropriate temperature and environment can recover the lattice damage and activate the RE emission [1,2].

In this research work, we investigate the post-implantation damage of two matrices of WBO materials, $\beta\text{-Ga}_2\text{O}_3$ and ZnO , implanted with RE to a fluence of 5×10^{14} , 1×10^{15} and 3×10^{15} atoms/ cm^2 and post annealed in O_2 , N_2 and Ar atmosphere. The effect of implantation and annealing on both crystal lattices was investigated by RBS/c technique. Aligned RBS spectra of the implanted $\beta\text{-Ga}_2\text{O}_3$ exhibited an increase in the damage peak with the fluence, which later on decreased after thermal annealing. On the other hand, implanted ZnO presented an increase in the damage peak that shifted towards lower energy for a higher fluence of 3×10^{15} atoms / cm^2 . After annealing in different atmospheres, the intensity of the damage peak decreased for all used fluences, while the intensity of the RE peak depended on the used atmosphere. Moreover, the level of crystal lattice damage caused by implantation with the same RE fluences in the case of $\beta\text{-Ga}_2\text{O}_3$ seems to be higher.

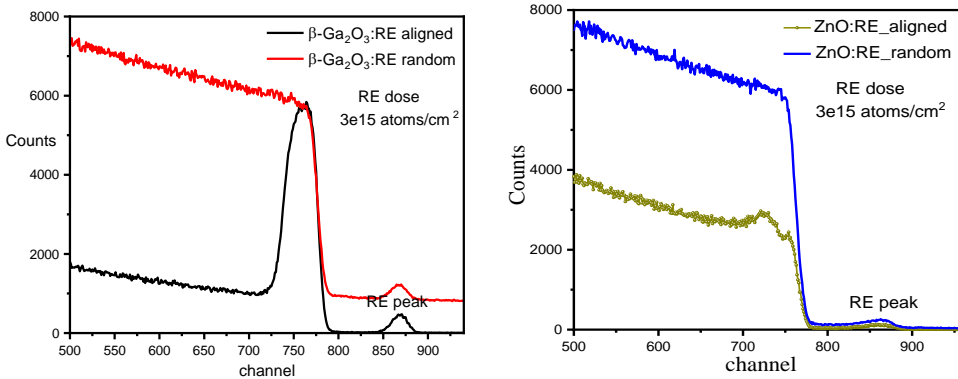


Figure 1 Random and aligned RBS spectra for $\beta\text{-Ga}_2\text{O}_3$ and ZnO implanted with RE

Acknowledgement. The work was supported by the international project co-financed by the funds of the Minister of Science and Higher Education in years 2021-2023;

contract No. 5177/HZDR/2021/0 and Helmholtz-Zentrum Dresden-Rossendorf (20002208-ST).

References

- [1] K. Lorenz et al., *Proc. of SPIE* 8987 (2014)
- [2] R. Ratajczak et al., *Appl. Surf. Sci.* 521 (2020)

Investigation of beryllium diffusion for various crystallographic directions in GaN grown by HVPE

Sierakowski K.¹⁾, Jakiela R.²⁾, Sochacki T.¹⁾, Iwinska M.¹⁾, Jaroszynski P.¹⁾, Fijalkowski M.¹⁾, Turek M.³⁾, and Bockowski M.¹⁾

¹⁾*Institute of High Pressure Physics, Polish Academy of Sciences, Warsaw, Poland*

²⁾*Institute of Physics, Polish Academy of Sciences, Warsaw, Poland*

³⁾*Institute of Physics, Maria Curie-Skłodowska University, Lublin, Poland*

Gallium nitride (GaN) is nowadays considered to be one of the most significant materials for fabrication of electronic and optoelectronic devices. A very convenient method for selective area doping is ion implantation. In order to obtain p-type the implanted acceptors have to be activated. Additionally, post-implantation damage in the crystallographic structure has to be removed. Both can be accomplished by high-temperature annealing of a sample. However, such treatment also results in the diffusion of the implanted element. In this work diffusion of Be was investigated for the main crystallographic directions in GaN: [0001], [10-10], and [11-20]. GaN layers were grown by halide vapor phase epitaxy (HVPE) in the mentioned above polar and non-polar directions on ammonothermal GaN seeds of the highest structural quality. Beryllium was implanted into the samples at room temperature with a dose of $2.9 \times 10^{15} \text{ cm}^{-2}$ and energy of 200 keV. Ultra-high-pressure annealing (UHPA) was performed to repair the post-implantation damage and activate the dopants [1]. Depth profiles of Be and atmospheric impurities (oxygen, hydrogen, and carbon) were measured by secondary ion mass spectrometry. A significant anisotropy of Be diffusion was measured for different crystallographic directions. The correlation between the maximum Be solubility and oxygen concentration in the samples was observed. The diffusion coefficients were calculated and summarized in an Arrhenius plot: $D(1/T)$. From this relation values of the pre-exponential factor D_0 and the activation energy were calculated.

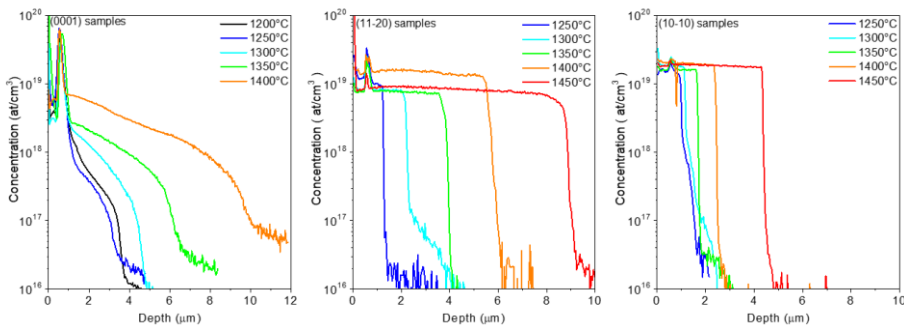


Figure 1. Be depth profiles measured by SIMS for [000-1], [11-20] and [10-10] crystallographic directions.

References

- [1] K. Sierakowski, R. Jakiela, B. Lucznik, P. Kwiatkowski, M. Iwinska, M. Turek, H. Sakurai, T. Kachi, M. Bockowski, *Electronics (Switzerland)*, **9**, 1380 (2020)

Structural degradation in graphite after argon ion irradiation investigated with Raman imaging

Gawęda M., Wilczopolska M., Suchorab K., Frelek-Kozak M., Kurpaska Ł., Józwiak I., Jagielski J.

NOMATEN Centre of Excellence, NOMATEN MAB, National Centre for Nuclear Research, 7 Andrzeja Soltańska Street, 05-400 Otwock, Poland

The awareness of the negative environmental changes induced by human activities pressures the quest for highly efficient green and low-emissive energy sources. That points the interest to the 4th generation high-temperature gas-cooled nuclear reactors (HTGR). Their concept is especially desirable due to the security of use through inhibiting nuclear reaction in temperatures reaching the maximum HTGR operation temperature. It is established by specific block construction with its main compound – graphite. However, the specific values of graphite's parameters depend strongly on the material's structure and purity. It is essential to establish the required level of structural order, defects and inhomogeneity. In the study, the pristine material was irradiated with energetic Ar⁺ ions with fluencies ranging from 10¹² up to 2×10¹⁷ ion/cm² to simulate the structural damage due to neutron irradiation. As the method of evaluation, Raman imaging was chosen for surface and in-depth mapping. Its sensitivity to subtle structural changes discloses the differences between particular samples and discrepancies inside them. The examination showed that the structural degradation gradually rises at the beginning while the specific point transition occurs and high level of degradation appears. Moreover, metal oxide impurities have been detected in the material in several places. Obtained results will indicate the applicability and service life of the examined material.

Acknowledgments

We acknowledge support from the European Union Horizon 2020 research and innovation program under NOMATEN Teaming grant (agreement no. 857470), from the European Regional Development Fund via the Foundation for Polish Science International Research Agenda PLUS program grant No. MAB PLUS/2018/8, and from Ministry of Education and Science founder of the „HTGR” project (agreement no. 1/HTGR/2021/14).

POSTER PRESENTATIONS

The effect of carbon ion implantation and xenon irradiation on tribological properties of titanium and Ti6Al4V alloy

Budzyński P.¹⁾, Kamiński M.¹⁾, Surowiec M.²⁾, Turek M.²⁾, Wiertel M.²⁾, Skuratov V.A.³⁾

¹⁾Lublin University of Technology, Nadbystrzycka 36, 20-618 Lublin, Poland

²⁾Institute of Physics, M. Curie-Skłodowska University, M. Curie-Skłodowska 1, 20-031 Lublin, Poland

³⁾Joint Institute for Nuclear Research, Joliot-Curie 6, 141980, Dubna, Russia

Titanium and its alloys are structural materials used for the construction of devices operating in space, aviation and nuclear reactors, where there is a high intensity of ionizing radiation. Due to its good mechanical properties and corrosion resistance, titanium can be used to build the new generation of accelerators with high swift ion flux. However, it has poor tribological properties. Various methods are used to improve tribological properties, including ion implantation. The effect of carbon ion implantation with an energy of 120 keV and xenon ion irradiation with an energy of 160 MeV on tribological properties of titanium and its Ti6Al4V alloy was studied. The aim of the work was to check whether there is a synergy between defects generated during nuclear S_n energy losses of implanted carbon ions and defects dominating during electron S_e energy losses caused by xenon ion irradiation. Friction factor and wear measurements were carried out during a tribological test under technically dry friction conditions on a pin/ball-on type Nano Tribometer NTR² from Anton Paar (CFM Instrument). The counterexample was a ball of 100Cr6 bearing steel with a diameter of $\varphi = 2$ mm, the contact force was 300 mN. Wear of the tested samples was measured as the cross-sectional area of the wear track on the surface of the sample. The wear tracks were measured using the Intra Form Talysurf profilometer and the Talymap Lite V7 software. Microphotographs of the sample surface were taken with a AFM and Tescan Vega 3LMU scanning electron microscope (SEM) equipped with X-ray microanalysis EDS and WDS systems.

Carbon implantation increases the friction factor of titanium and eliminates oscillatory changes in the friction coefficient of titanium at a depth 25 times greater than the range of implanted ions. The average oxide content in the trace of the sample implanted with a dose of $1 \times 10^{17} \text{ C}^+/\text{cm}^2$ is slightly higher than their content in the unimplanted sample and increases after xenon irradiation. The contribution of oxidative wear is increasing, which is facilitated by the penetration of oxygen into the sample along the radiation damage and the cavities on the surface of the sample created during irradiation. Irradiation of carbon-implanted titanium restores the oscillatory changes in the friction factor characteristic of the not implanted samples above 1200 tribological test cycles.

Carbon implantation causes a decrease in the friction coefficient of the Ti6Al4V alloy, the greater the higher the dose of the implanted carbon ions. The dose of $1 \times 10^{17} \text{ C}^+/\text{cm}^2$ results in a 3-fold reduction in wear compared to a not implanted samples. Oxidative wear dominates. Irradiation of Ti6Al4V alloy implanted with carbon ions leads to an increase in the friction coefficient. Irradiation destroys the DLC layer formed on the Ti and Ti6Al4V surface. The synergy effect of changes in tribological properties of titanium and its Ti6Al4V alloy caused by carbon ion implantation and xenon irradiation was not observed.

Defects studies of gold exposed to Au and H implantation

Horodek P.¹⁾, Siemek K.¹⁾, Skuratov V.A.²⁾

¹⁾*Institute of Nuclear Physics, Polish Academy of Science, Krakow 31-342, Poland*

²⁾*Joint Institute for Nuclear Research, Dubna 141980, Russia*

We report experimental studies of silver after 167 MeV Xe²⁶⁺ ions irradiation. Heavy ion implantation of samples with fluences 10^{12} , 2×10^{12} , 5×10^{12} , 10^{13} , 5×10^{13} and 10^{14} cm⁻² was performed. Radiation damage was investigated with variable energy positron beam (VEP). Doppler broadening spectroscopy (DB) was applied and the line shape

S parameter of annihilation line was extracted. The analysis of S parameter profiles gives information about the presence of open volume defects in irradiated samples. The positron diffusion length extracted from the profile decreases with the fluence increase. It points out the increase of defects concentration. Probably, changes in the size or type of defects generated by various fluences took place.

AC conductivity of Ti-Zr-C hard nanocomposite coatings

*Gałasziewicz P. and Koltunowicz T.N.**Lublin University of Technology, Nadbystrzycka 38D, 20-618 Lublin, Poland*

Nanocomposites based on hard compounds are currently on the stage of active research and development. Hence the analysis of a relation between nanostructure and functional properties is of great importance.

Ti-Zr-C coatings were obtained by sputtering with two-target DC magnetron onto Si substrates. Alternating current properties of Ti-Zr-C nanocomposites samples were tested on the stand specifically described in [1]. The stand was equipped with CS 204AE-FMX-1AL helium cryostat (Advanced Research Systems, USA). Measurements of alternating current characteristics (conductivity σ and phase angle φ) were carried out in a temperature range from 20 K to 375 K and in the frequency range from 50 Hz to 5 MHz.

The analysis reveals the nature of tunnelling conductance between the nanoparticles. On the computer simulation of the frequency dependence of the frequency coefficient, three maxima were discovered. Two of them were attributed to dominant phases (Ti_{1-x}Zr_x)C and amorphous carbon (a-C). The third one is related to the content of another type of nanophase that, due to low content, could not be determined by structural methods. Tests showed promising results in suitability for micromechanical devices, in particular: sensors, actuators, power-producing devices. These findings establish an understanding of microstructural regularities and enlarge the potential application space for TiZrC-based systems.

References

- [1] Koltunowicz T N , J. Apps. Spectrosc. 2015;82:653-658.

TiAlN coatings blistering under high-temperature Ar⁺ ion irradiation

*Komarov Fadei F.¹⁾, Konstantinov Stanislav V.¹⁾, Żuk Jerzy²⁾, Chizhov Igor V.³⁾,
Zaikov Valery A.³⁾*

¹⁾*A.N. Sevchenko Institute of Applied Physical Problems of Belarusian State University, 7 Kurchatov street, 220045 Minsk, Belarus*

²⁾*Institute of Physics, Maria Curie-Skłodowska University, Pl. M. Curie-Skłodowskiej 1, 20-031 Lublin, Poland*

³⁾*Belarusian State University, 4 Nezavisimosti Avenue, Minsk 220030, Minsk, Belarus*

Radiation tolerant materials and coatings are perspective for use in nuclear energetics and spacecrafts. In nuclear reactors, they can be exploited as fuel claddings and other different constructions. For spacecrafts, they are effective in saving electronics from the cosmos corpuscular irradiation. Nanostructured TiAlN coatings were deposited on the AISI 304 stainless steel substrates by reactive magnetron sputtering. Samples were irradiated by Ar⁺ ions with an energy of 200 keV in the fluence range from $2.5 \cdot 10^{16}$ ion/cm² to $2 \cdot 10^{17}$ ion/cm² at a temperature of 480 °C. Coatings elemental composition, structural-phase state as well as mechanical properties were investigated. The impact strength of the TiAlN films under study was calculated as the H/E* ratio. It has been found that nanostructured TiAlN coatings are radiation-resistant up to the irradiation fluence of $2 \cdot 10^{17}$ ion/cm², at which the onset of segregation of the (Ti, Al)N solid solution as the main phase of the coatings and their blistering is observed.

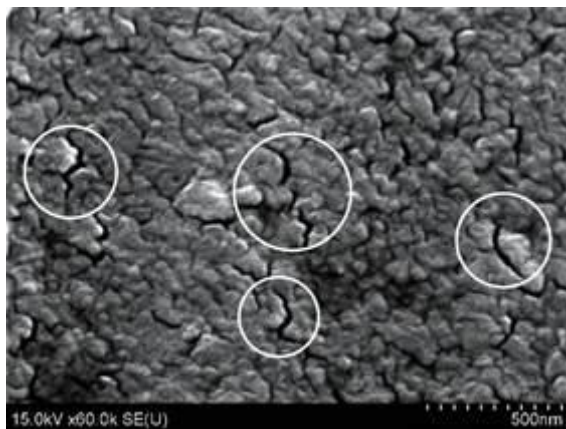


Figure 1: SEM image of TiAlN coatings blistering under 200 keV Ar⁺ $2 \cdot 10^{17}$ ion/cm² at 480 °C.

Effect of atmospheric plasma spraying parameters on cavitation erosion and wet-environment tribological behaviour of Al₂O₃-13% TiO₂ coatings

Szala Mirosław¹⁾, Kamiński Mariusz²⁾, Łatka Leszek³⁾

¹⁾Department of Materials Engineering, Faculty of Mechanical Engineering, Lublin University of Technology, Nadbystrzycka 36D, 20-618 Lublin, Poland

²⁾Department of Automotive Vehicles, Faculty of Mechanical Engineering, Lublin University of Technology, Nadbystrzycka 36D, 20-618 Lublin, Poland

³⁾Faculty of Mechanical Engineering, Wrocław University of Science and Technology, Łukasiewicza 5, 50-371 Wrocław, Poland

Atmospheric plasma spraying (APS) is an up-to-date technology systematically developed. One of the crucial ideas is to inject the sprayed feedstock powder internal or external into the plasma arc. Spraying parameters affects the microstructure and properties of the coating, which decides the operation performance of coatings and specific machine components. In this work, the alumina-titania (Al₂O₃-13% TiO₂) coatings were deposited on X5CrNi10-10 stainless steel using APS method. The internal and external injection spraying mode, constant spray velocity (500 mm/s) and two spray distances to the substrate, namely 80 mm and 100 mm were employed. The microstructure and hardness of the deposited coatings were studied. Cavitation erosion resistance was estimated using ASTM G32 method. Sliding wear resistance was estimated in a distilled water environment using ball-on-disc apparatus. The wear results were analysed to coatings properties and APS spray parameters. Results indicate that spray parameters affect erosion and tribological results. A shorter spraying distance indicates higher coatings uniformity, while increasing distance lowers the hardness and porosity. Coating fabricated with 80 mm spray distance with internal method has the superior tribological performance.

Influence of energy and mass of ion on $\text{TiO}_2/\text{SiO}_2$ bilayer mixing

Phuc T.V.^{1,2)}, Kulik M.^{2,3)}, Khiem L.H.¹⁾, Tuan P.L.^{2,4)}, Tiep N.V.^{1,5)}, Tuyen L.A.⁶⁾, Doroshkevich A.^{2,7)}, Madadzada Afag^{2,8)}

¹⁾*Institute of Physics, Vietnam Academy of Science and Technology, 18 Hoang Quoc Viet, Cau Giay, Ha Noi, Viet Nam*

²⁾*Frank Laboratory of Neutron Physics, Joint Institute for Nuclear Research, 141980 Dubna, Russia*

³⁾*Institute of Physics, Maria Curie-Skłodowska University, pl. M. Curie-Skłodowskiej 1, 20-031 Lublin, Poland*

⁴⁾*Vietnam Atomic Energy Institute, 59 Ly Thuong Kiet, Hoan Kiem, Hanoi, Vietnam*

⁵⁾*Flerov Laboratory of Nuclear Reactions, JINR, 141980 Dubna, Moscow Reg., Russia*

⁶⁾*Center for Nuclear Technology, Vietnam Atomic Energy Institute, Ho Chi Minh City 700000, Viet Nam*

⁷⁾*Donetsk Institute for Physics and Engineering named after O.O. Galkin, 03028, Nauki ave., 46 Kiev, Ukraine*

⁸⁾*Department of Neutron Physics, National Nuclear Research Centre JSC, Baku-Shamahi hw 20km, AZ 0100 Baku, Azerbaijan.*

The ion beam-induced mixing has been commonly applied to create stable, metastable, amorphous, and crystalline phases in bilayer and multilayer materials. It has been known well that there exists an optimum combination of thickness of the over-layer thin film and the ion beam parameters to enhance the interfacial mixing yield, whereas the dependence of mixing amount on ion fluence and deposited energy can be predicted using mixing models. Nevertheless, the precise recipe for finding the optimum combination and understanding the modification of the parameters in the mixing models are still under development. The main difficulty comes from the fact that the mixing depends not merely on ion energy and mass. Influence of these beam parameters on mixing could thus be characterized only by the primary parameters that can be measurable using experimental technique. The present work is aimed to obtaining a better understanding for the behaviour of the mixing as a function of ion energy and mass, and the relative roles of kinetics in the bilayer mixing. Towards this target, the atomic mixing of $\text{TiO}_2/\text{SiO}_2$ system was conducted with the noble gas ions Ne^+ , Ar^+ , Kr^+ , Xe^+ at different energies of 100, 150, 200, 250 keV. The RBS method was used for determining the elemental depth profiles of the samples. Shifting of the Ti, Si energy edges from RBS spectra indicated that the mixing of the atoms across the interface of systems led to forming of the transition area between the layers. Mixing amount was quantified by changing thickness of $\text{TiO}_2/\text{SiO}_2$ transition layers. It has been found that the dependence of the mixing on energy as a simple linear function for all ion species with cascade mixing is dominant in the studied energy range. The mixing degree is not proportional to the defect concentration, whereas the ion energy transferring to the target atoms created deeper damage plays a crucial role in broadening of $\text{TiO}_2/\text{SiO}_2$ mixed area. Mixing amount strongly depends on the ion mass, it was observed that relative thickness of mixed layers increases 2.8 and 7.6 times higher for Kr and Xe, respectively, in comparison with that of Ne. The fast increase of the ion density in the mixed layers showed a major contribution in broadening of the $\text{TiO}_2/\text{SiO}_2$ mixed layers instead of the linear growth in nuclear energy loss.

Molecular dynamics simulations of primary radiation damage in Silicon Carbide

Kucal E.¹⁾, Czerski K.^{2,3)}, Koziol Z.¹⁾

¹⁾National Centre for Nuclear Research, NOMATEN CoE MAB+ Division, A. Soltana 7, 05-400 Otwock, Poland

²⁾Institute of Physics, University of Szczecin, 70-451 Szczecin, Poland

³⁾Institut für Festkörper-Kernphysik gGmbH, Leistikowstraße 2, 14050 Berlin, Germany

Molecular dynamics simulations provide information on atomic displacement cascades on time dependence and account for the effects of crystal structure and temperature. In this work, molecular dynamic simulations in LAMMPS of low energy ion irradiation of cubic silicon carbide will be presented. During passage through matter, ions lost their energy due to atomic collision and electronic excitation. In low energy regimes, elastic collisions are dominant and in many cases, electronic stopping is neglected. Here, MD simulations are performed with and without adding the electronic stopping effects. The results show the differences with number of vacancy in both case.

Orientation dependence of RT stabilized SHI induced tetragonal tracks in a ZrO_2 monoclinic matrix

Lee M.E.¹⁾, O'Connell J.¹⁾ and Skuratov V.²⁾

¹⁾Centre for HRTEM, Nelson Mandela University, Gqeberha 6031, South Africa

²⁾FLNR, JINR, Dubna, Russia

Pure bulk zirconia (ZrO_2) is a polymorphic oxide that exists in three different low pressure crystal structures below its melting point namely, the high temperature phases cubic and tetragonal as well as the low temperature monoclinic phase [1]. Irradiation of bulk natural zirconia at room temperature along the monoclinic $[100]_m$ crystal axis were shown by transmission electron microscopy to produce non-continuous tetragonal latent tracks consisting of segments approximately 30 nm in length and rectangular cross sections of the order 2.5 nm. The segments were aligned along the $[001]_t$ crystal axis and approximately 9° to the $[100]_m$ axis. It was suggested that the mechanism for the stabilization of the high temperature phase could be due to the surface energy of the interface surfaces [3] or the presence of additional vacancies and interstitial oxygen atoms [4]. In this presentation we present results for irradiated bulk monoclinic zirconia along different crystalline directions to determine the influence of interfacial surfaces on the formation and stabilization of latent tracks.

Individual ion tracks were found to be composed of the high temperature stable tetragonal phase. The c axis of the monoclinic and tetragonal regions was parallel with 45° relative rotation about the c axis. Discontinuities in the tetragonal phase together with a slight misalignment relative to the ion path was ascribed to the difference in a-c angle between the tetragonal and monoclinic phase.

References

- [1] J.E. Bailey, Proc. R. Soc. A. Math. Phys. Sci., 279 (1964) 395-412
- [2] J.H. O'Connell, M.E Lee, V.A Skuratov and R.A. Rymzhanov, Nucl. Inst. Meth. Phys. Res. B, 473 (2020) 1-5
- [3] M.W. Pitcher, S.V. Ushakov, A. Navrotsky, B.F. Woodfield, G. Li, J. Boerio-Coates and B.M. Tissue, J. Am. Ceram. Soc., 88 (2005) 160-167
- [4] X. Lu, K. Liang, S. Gu, Y. Zheng and H. Fang, J. Mater. Sci., 32 (1997) 6653-6656

Structure and magnetic properties of Ni-doped tin oxide films

*Ksenevich V.K.¹⁾, Dorosinets V.A.¹⁾, Adamchuk D.V.¹⁾, Samarina M.A.¹⁾,
Lyubchik A.I.²⁾*

¹⁾*Belarusian State University, Nezalezhnastsi ave. 4, 220030 Minsk, Belarus*

²⁾*Research Centre in Industrial Engineering Management and Sustainability, Lusófona University, Campo Grande, 376, 1749-024 Lisboa, Portugal*

Possibility of application of diluted magnetic semiconductor oxides in spin-based electronics is actively discussed during last decades [1]. Different methods are used for synthesis of metal oxide semiconductors doped with ferromagnetic atoms. Ni-doped tin oxide films in our study were fabricated by DC magnetron sputtering of tin target with Ni inserts in argon-oxygen plasma with an oxygen content in the range of 0-6 vol. % followed by 2-stage annealing procedure in air. Variation of oxygen content in argon-oxygen plasma strongly affects structural properties of tin oxide films [2]. Raman spectral-analytical system Nanofinder HE was used for characterization of structure of Ni-doped tin oxide films. Magnetization measurements were carried out using closed-cycle Helium refrigerator CFHF Cryogenics Ltd. in the temperature range of 4-300 K and in magnetic field up to 8 T.

Analysis of the Raman spectra of Ni doped tin oxide films reveals an amorphization process with increase of oxygen content in the plasma during magnetron sputtering process. S-shaped form of magnetization curves indicates superposition of dia- and ferromagnetic components in the samples. Anhysteretic form of magnetization curves of the films indicates superparamagnetic behavior of Ni-doped tin oxide films. The relative part of the ferromagnetic component gradually increases with the temperature decreasing.

References

- [1] Gupta A, Zhang R, Kumar P, Kumar V, Kumar A, Magnetochemistry 2020;6:15.
- [2] Adamchuk D, Ksenevich V, Poklonski N, Navickas M, Banys J, Lithuanian Journal of Physics 2019;59:179.

Formation of ZnSe nanoclusters in silicon dioxide layers by high-fluence ion implantation: Experimental data and simulation results

Makhavikou Maksim¹⁾, Komarov Fadei¹⁾, Komarov Alexandr¹⁾, Miskevich Sergei¹⁾, Milchanin Oleg¹⁾, Parkhomenko Irina²⁾, Żuk Jerzy³⁾, Romanov Ivan²⁾ and Wendler Elke⁴⁾

¹⁾A.N. Sevchenko Institute of Applied Physics Problems, Kurchatov Str. 7, 220045 Minsk, Belarus

²⁾Belarusian State University, Independence Ave. 4, 220030 Minsk, Belarus

³⁾Maria Curie-Skłodowska University, Pl. M. Curie-Skłodowskiej 1, 20-031 Lublin, Poland

⁴⁾Friedrich-Schiller University Jena, Max-Wien-Platz 1, D-07743 Jena, Germany

In this study, thin layers of SiO₂ (600 nm) were implanted at 550°C with Zn⁺ (150 keV, 4×10^{16} cm⁻²) and Se⁺ (170 keV, 4×10^{16} cm⁻²) ions. The combination of elemental analysis (RBS) and structural (RS, TEM) techniques have been used to identify the phases of the formed ZnSe/SiO₂ nanocomposite. A theoretical model was developed for simulating high-fluence implantation of two types of atoms to form ZnSe compound nanoclusters in a silicon dioxide matrix. The model is based on solving a set of the convection – diffusion – reaction equations [1].

Using the methods of TEM and RS, it is found that ZnSe nanoclusters are crystalline and have a mean diameter of 5 nm and are distributed with a density of 1.15×10^{12} cm⁻². From the theoretical and experimental data, the mean values of the radiation-enhanced diffusion coefficients for zinc ($D_{\text{Zn}} = 1.94 \times 10^{-16}$ cm²/s) and selenium ($D_{\text{Se}} = 2.88 \times 10^{-16}$ cm²/s) in silicon dioxide were determined. It was found that ~ 6.2 at. % of the selenium atoms implanted at 550°C combine with preimplanted zinc atoms, that is, produce crystalline ZnSe nanoclusters. This indicator is approximately comparable to the value of ~ 5.6 at. % obtained experimentally by analyzing TEM images. Optical properties of the formed nanocomposite layers are discussed as well.

References

- [1] Komarov A, Komarov F, Milchanin O, Vlasukova L, Parkhomenko I, Mikhailov V, Mokhovikov M, Miskevich S, Technical Physics; 2015;60;9:1335.

Simulation of coimplantation of boron and carbon in silicon

Miskiewicz S., Komarov A., Komarov F.

Institute of Applied Physics Problems, 220045 Minsk, Belarus

Boron diffusion in Si during the RTA after ion implantation is significantly accelerated due to high concentration of Si-interstitials (TED). To reduce TED, the implantation of C which binds the interstitials is used [1]. Optimal concentration of C in Si is 1 C-atom to 1.15 interstitials [2]. The model of coimplantation is developed. The results of simulation is shown in Fig. 1 and match well with experiments [2-5].

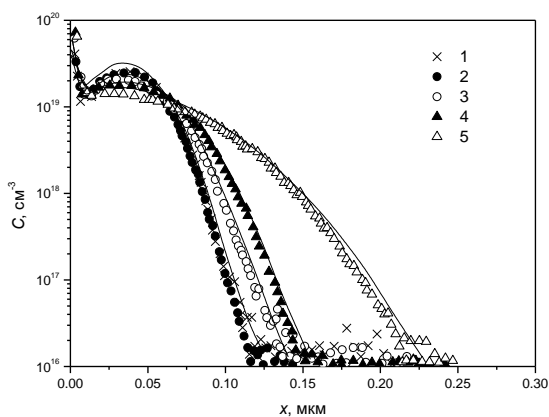


Figure 1: Boron profiles before (1) and after annealing 900°C 30 s with (2) and without (3) carbon, 1100°C 30 s with (5) and without (6) carbon. Solid lines are results of simulation.

References

- [1] Liao H.-C., Lin J.-C., Chang R.-D., Japanese J. Appl. Phys. 2018; 57:8.
- [2] Cowern N.E.B., Cacciato A., Custer J.S. et al., Appl. Phys. Lett. 1996; 68:8.
- [3] Jain S.C., Schoenmaker W., Lindsay R. et al., J. Appl. Phys. 2002; 91:11.
- [4] Vanderpool A., Taylor M., Nucl. Instr. and Meth. 2005; 237.
- [5] Mirabella S., De Salvador D. et al., Nucl. Instr. and Meth. 2004; 216.

Structural ordering of magnetic nanoparticles in aqueous media by small-angle neutron scattering

Nagornyi A.V.¹⁾, Shlapa Yu.Yu.²⁾, Belous A.G.²⁾, Vekas L.³⁾, Bulavin L.A.¹⁾

¹⁾Taras Shevchenko National University of Kyiv, Volodymyrska Str. 60, 01601 Kyiv, Ukraine

²⁾V.I.Vernadsky Institute of general and inorganic chemistry, Academician Palladin Ave. 32/34, 03142 Kiev, Ukraine

³⁾Romanian Academy-Timisoara Branch, Center for Fundamental and Advanced Technical Research, Laboratory for Magnetic Fluids, 300222 Timisoara, Romania.

Magnetic fluids (MFs) are unique artificial colloidal systems combining magnetic properties and fluidity. They consist of magnetic nanoparticles (MNPs) with a characteristic size of about 10 nm dispersed into a liquid medium. Colloidal stability of the MNPs in the liquid carrier is reached by steric repulsion between the surfactant coatings adsorbed on the MNPs' surfaces. The study of MFs is of great practical and fundamental importance. In recent years, much attention aimed at the bulk structure of magnetic fluids at various conditions, which is well observed by small-angle neutron scattering (SANS) [1]. In the case of water based MFs, with many applications in biotechnology and biomedicine [2-4], MNPs have to be nanosized, monodispersed, nontoxic and have stability to aggregation due to effective-hydrophilic coatings. Colloidal aggregation cannot be avoided completely in water-based magnetic fluids [5,6]. The issue of aggregation becomes especially important in biorelevant solutions, which are naturally water-based.

The reason for aggregation in an aqueous medium is the dominance of the energy of interaction between particles over the energy of thermal motion in the medium that is especially pronounced for magnetic NPs. This work considers structural studies of aqueous magnetic fluids and aqueous dispersions with nonmagnetic nanoparticles basing par excellence on small-angle neutron scattering techniques as powerful tool in condensed matter science.

References

- [1] Petrenko V.I., Nagornyi A.V., Gapon I.V., et al., Selected Reviews Springer Proceedings in Physics (eds. Leonid Bulavin and Alexander Chalyi), Ch.10, 205-229, (2018).
- [2] Socoliuc V., Davide Peddis, Viktor Petrenko, et al., Magnetochemistry. 6(1), (2020) 1-36.
- [3] Krasia-Christoforou T., et al., Nanomaterials. 10(11), (2020) 1-67.
- [4] Siposova K., et al., ACS Applied Bio Materials. 2(5), (2019) 1884-1896.
- [5] Nagornyi A.V., et al., J. Mag. Mag. Mater. 501, (2020) 166445.
- [6] Nagornyi A.V., et al., Journal of Molecular Liquids. 312, (2020) 113430.

Microstructure, chemical bonding and tribo-mechanical properties of Ti-Zr-Mo-C

Pogrebnjak A.D.¹⁾, Ivashchenko V.I.²⁾, Budzyński P.³⁾, Kamiński M.³⁾

¹⁾Sumy State University, 2, Rymskogo-Korsakova Str, 40007 Sumy, Ukraine

²⁾Frantsevich Institute for Problems of Materials Sciences, NAS of Ukraine, 3 Krzhizhanovsky Str., 03142 Kyiv, Ukraine

³⁾Faculty of Mechanical Engineering, Lublin University of Technology, Nadbystrzycka 36, 20-618 Lublin, Poland

Surface thin films have been used as protective and functional layers in various engineering fields for many years. The current trend for PVD technology is to develop transition metal carbides (TMC) films. It has been learned that TMC films show improved strength, toughness, wear-resistance, chemical inertness and conductivity [1]. Niobium is a corrosion-resistant material which is expected to be biocompatible in the living body. Niobium, when alloyed with titanium or zirconium can produce, in the proper concentration, a super-conducting metal, and is thus used primarily in non-medical applications. The presence of zirconium in niobium results in higher mechanical properties. The addition of titanium to niobium reduces the melting temperature making it easier to process. The presence of titanium in niobium can also improve corrosion resistance, particularly in lower pH environments [2]. Titanium and zirconium also reduce the melting temperature of niobium and improve the ability of molybdenum to mix during melting. Because niobium and zirconium are closer in density to molybdenum, the last has a reduced tendency to segregate during melting [3]. Considering all factors mentioned above, the combination Ti-Zr-Mo with C can produce a hard, abrasion-resistant, inert, ceramic material.

Herein, thin Ti-Zr-Mo-C films have been deposited onto Si (100) substrates by direct-current magnetron sputtering and studied with respect to the stability of the structural and functional properties using the most commonly used methods.

The main experimental results of Ti-Zr-Mo-C films are: (1) stable Ti-C, Zr-C, Mo-C and C-C bonds are identified and the solid solution (Ti,Zr,Mo)C is formed, therefore, the film structure can be presented as the nanocrystals of above solid solution surrounded by a-C phase; (2) Knoop hardness steadily increased with increasing sputtering current at the graphite target to 250 mA reaching the maximum value of about 35 GPa; (3) the structure and properties of sputter-deposited metal carbide films are precisely controlled by composed with appropriate elements. The transition metals such as Zr and Mo have a strong effect on binary TiC films, due to their lower carbon affinity and their tendency to form complex crystal structures.

First-principles study of defect formation and migration in nano size TiC crystal under ions irradiation

Popov E.P.^{1,2,3)}, Mirzayev M.N.^{3,4,5)}, Donkov A.A.^{1,3)}, Hussien M.A.M.⁶⁾,
Obiedallah F.M.H.⁶⁾, Anatolievich S.A.³⁾, Horodek Pawel⁷⁾

¹⁾Georgi Nadjakov Institute of Solid State Physics, Bulgarian Academy of Sciences, 1784, Sofia, Bulgaria

²⁾Institute for Nuclear Research and Nuclear Energy, Bulgarian Academy of Sciences, Sofia, 1784, Bulgaria

³⁾Joint Institute for Nuclear Research, Dubna, Moscow distr., 141980, Russia

⁴⁾Institute of Radiation Problems, Azerbaijan National Academy of Sciences, Baku, AZ1143, Azerbaijan

⁵⁾Azerbaijan State Oil and Industry University, Scientific-Research Institute Geotechnological Problems of Oil, Gas and Chemistry, AZ1010 Baku, Azerbaijan

⁶⁾Faculty of Science, Assiut University, Assiut, Egypt

⁷⁾Institute of Nuclear Physics, Polish Academy of Science, Krakow 31-342, Poland

In the present work, according to positron life time calculation we used MIKA package with LDA which gave regular and self-consistent schemes without relaxation for nano TiC crystals. The nano crystal TiC unit cell parameters were fixed a , b , $c = 4.3305 \text{ \AA}$ and $\alpha, \beta, \gamma = 90^\circ$, as it has FCC crystal structure with Fm/3m (225) group symmetry in Hermann-Mauguin notation. To organize the lattice of TiC in MIKA we employed structure composed of 500Ti+500C atoms. The void cluster increases to two vacancies. We investigated this more efficiently with MIKA carrying out the calculations with MIKA without relaxations, although the H and He atoms have been moved to locations that can be occupied owing to hydrogen-hydrogen chemical bonds. The positron life time (PLT) of perfect TiC materials is 111.87 ps as obtained from MIKA through local density approximation (LDA). But one can note that this time is increased to 180.07 ps for one vacancy Ti existing in the TiC crystal structure. So, this is a good evidence that the PLT increased by increasing the number of Ti vacancies. When the Ti vacancy is replaced by C vacancy also the PLF increases but in a different way.

Investigation of zinc diffusion for various crystallographic directions in GaN grown by HVPE

Sierakowski K.¹⁾, Jakiela R.²⁾, Sochacki T.¹⁾, Iwinska M.¹⁾, Jaroszynski P.¹⁾, Fijalkowski M.¹⁾, Turek M.³⁾, and Bockowski M.¹⁾

¹⁾*Institute of High Pressure Physics, Polish Academy of Sciences, Warsaw, Poland*

²⁾*Institute of Physics, Polish Academy of Sciences, Warsaw, Poland*

³⁾*Institute of Physics, Maria Curie-Skłodowska University, Lublin, Poland*

Ion implantation (I/I) seems to be nowadays one of the most important techniques for manufacturing gallium nitride (GaN) based semiconductor devices. High-energy ions might be implanted into crystals in order to create doped regions. To achieve the required conduction in the implanted layer, p-type or n-type, one must anneal the structure to activate the dopant. Temperature treatment is also required to remove the I/I-induced structural damage. In the case of GaN high-temperature annealing is difficult due to thermodynamics of GaN (thermal decomposition above 800°C in atmospheric pressure). Ultra-high-pressure annealing (UHPA), which involves high pressure of nitrogen, allows to avoid the decomposition of GaN samples. The most popular p-type dopant in GaN is magnesium (Mg). However, other elements are also investigated. One of other possible candidates for p-type doping is zinc (Zn) [1]. In the presented work GaN doping by Zn implantation was investigated. HVPE-GaN layers were grown on ammonothermal seeds of three polarities: (0001), (10-10), and (11-20). Zn I/I was performed with the energy of 230 keV and fluence of 10^{16} cm^{-2} . The samples were then treated with UHPA in the temperature range 1250°C÷1450°C for 30 and 240 minutes.

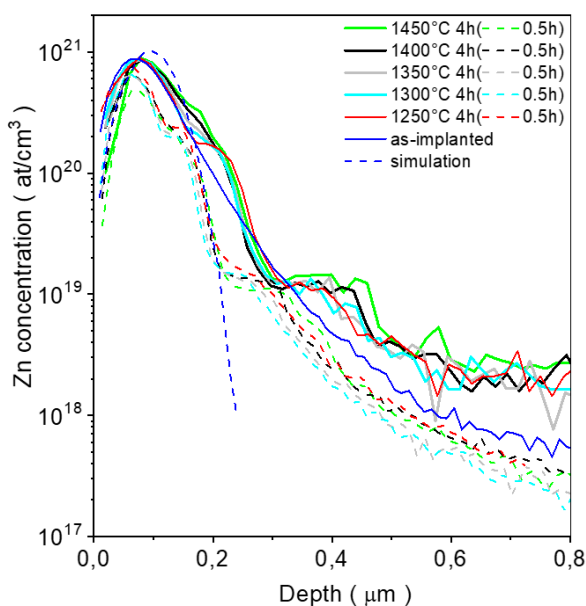


Figure 1. SIMS depth profiles of Zn in (11-20)-GaN annealed in ultra high pressure

A constant nitrogen pressure of 1 GPa was applied for all the annealing runs. X-ray diffraction measurements were employed to assess the success of structural damage removal by annealing. The depth profiles of Zn and atmospheric impurities were determined by secondary ion mass spectrometry (SIMS). This allowed to study the diffusion of the implanted element in GaN. An anisotropy of diffusion was observed for the different crystallographic directions.

References

- [1] M. Zajac, L. Konczewicz, E. Litwin-Staszewska, M. Iwinska, R. Kucharski, S. Juillaguet, and S. Contreras, J. Appl. Phys. 129, 135702 (2021)

Effect of nitrogen ion implantation on cavitation erosion resistance of Stellite 12 and Stellite 6 hardfacings

Szala Mirosław^{1)*}, Turek Marcin²⁾, Chocyk Dariusz³⁾, Skic Anna⁴⁾

¹⁾Department of Materials Engineering, Faculty of Mechanical Engineering, Lublin University of Technology, Nadbystrzycka 36D, 20-618 Lublin, Poland

²⁾Institute of Physics, Maria Curie-Skłodowska University in Lublin, Pl. M. Curie-Skłodowskiej 1, 20-031 Lublin, Poland

³⁾Department of Applied Physics, Faculty of Mechanical Engineering, Lublin University of Technology, Nadbystrzycka 36D, 20-618 Lublin, Poland

⁴⁾Department of Mechanical Engineering and Automatic Control, University of Life Sciences, Głęboka 28, 20-612 Lublin, Poland

The research of two stellite hardfacings namely, Stellite 12 and Stellite 6 layers were post-treated using nitrogen ion implantation and their cavitation erosion resistance was investigated. Paper studies the cavitation erosion resistance, deterioration behaviour and presents a phenomenological model of unimplanted and ion-implanted satellite hardfacings. Grounded and polished TIG-deposited layers were treated via nitrogen ion implantation by 120 keV N⁺ ions and fluence of $1 \times 10^{17} \text{ cm}^{-2}$. The microstructure, hardness and phase composition of hardfacings were studied. The cavitation erosion tests were conducted acc. ASTM G32 standard using stainless steel AISI 304 as a reference sample with the stationary specimens method. Cavitation experiments were done in distilled water and water slurry. The damaged surfaces of unimplanted and implanted coatings were qualitatively studied using atomic force microscopy (AFM), 3D roughness profilometer, scanning electron microscopy (SEM). Moreover, phase development due to ion-implantation and cavitation erosion were analysed using X-ray diffraction (XRD). Findings indicate the positive effect of ion implantation on the cavitation erosion resistance of stellites. Hardfacings presents almost 100 times higher resistance to cavitation than reference stainless steel specimens. The prolonged incubation period of cobalt coatings seems crucial for their superior anti-cavitation behaviour. Analysis of the cavitation curves, surface development, phase changes and microscopic studies allows elaborating the original model of implanted stellites cavitation erosion resistance.

Ionization in hot cavity ion sources

Turek M.

Maria Curie-Skłodowska University, Pl. M. Curie-Skłodowskiej 1, 20-031 Lublin, Poland

A theoretical model of ionization in a hot cavity is presented. It is based on discretisation of evolution of the system [1] and makes use of only a few parameters involving the size of the extraction opening, the increase of effective extraction opening size due to the extraction potential, the area of internal ionizer surface etc. The model enables fast calculation of evolution of the system as well as the total ionization efficiency. Some exemplary calculations show that total efficiencies achieved in the hot cavity depends on the effective size of the extraction opening (that includes effect of extraction voltage) and reaches values by far exceeding predictions of the Saha-Langmuir formula. Two different ways to describe the state of the system are considered. One of them is just the number of ions and neutrals in the cavity, the other is the total number of particles and a difference between neutral and ions numbers. Each of two descriptions has its advantages and depending on case may be more useful for description of evolution of the system. A four special cases/scenarios of ionization in hot cavity are considered: a closed cavity, a cold cavity, a case of weak extraction, and optimal "each ion scenario". For each of these cases the formulae describing the evolution are presented and different schemes of system behaviour are discussed. Moreover, the two latter cases formulae enabling calculations of total ionization efficiency are derived. Their predictions are compared to results of numerical calculations. The presented model gives opportunity of better understanding of dynamics of ionization processes that take place inside hot cavity ion sources.

References

[1] Latuszyński A., Pysznik K., Drożdżel A ,et al. *Vacuum* 2007;81:1150

Ionization of short-lived nuclides in a hot disc-shaped cavity

Turek M.

Maria Curie-Skłodowska University, Pl. M. Curie-Skłodowskiej 1, 20-031 Lublin, Poland

The numerical model of ionization in a disc-shaped cavity is presented [1]. The model takes into account nuclide losses due radioactive decay as well as delays related to the particle sticking to hot ionizer walls. Two different shapes of the ionizer cavity are studied. The flat disc cavity with large diameter seems much more suitable for stable but hard-to-ionize substances, as its shape makes the average number of collisions with the walls large by an order of magnitude that in the case of the compact cavity. On the other hand, the compact cavity is superior for short-lived isotopes, as the produced ions are extracted out of the cavity very fast. This is especially important for substances with the long average particle-wall sticking time - it has been proven that the efficiency of the compact cavity is almost unaffected by sticking delays up to 10 ms. The influence of the size of the extraction opening was also under investigation. It was found that enlarging the extraction channel diameter is a very simple way to increase the efficiency of the flat disc cavity for short-lived nuclides, especially those with small ionization coefficient. Current-voltage curves obtained for both configurations are characterized by different shapes. In the case of compact cavity one observes fast increase followed by saturation while for the flat disc cavity increase of extraction voltage induces larger current, though this effect is weaker for extraction voltages larger than 2 keV. The optimal value of extraction voltage for the compact cavity is near 0.5 kV, while for the flat disc cavity such value is much higher, approximately 2 kV.

References

[1] Turek M., *Devices and Methods of Measurements* 2020;11(2):132

Modification of optical electronic and microstructural properties of PET by 150 keV Cs⁺ irradiation

Musiatowicz M., Turek M., Drożdżiel A., Pysznia K., Grudziński W.

Maria Curie-Skłodowska University, Pl. M. Curie-Skłodowskiej 1, 20-031 Lublin, Poland

Thick (0.125 mm) sheet samples of PET were irradiated with 150 keV Cs⁺ ion beam with fluences in the range from 10¹³ cm⁻² up to 10¹⁶ cm⁻². Raman and UV-VIS spectroscopy measurements have shown destruction of numerous bonds within the polymer – this effect intensifies with fluence. Raman spectroscopy shows the presence of amorphous graphitelike structures as the broad G band appears in the spectrum. The analysis of absorbance spectra also confirms formation of numerous carbon clusters leading to a formation of vast conducting structures in the modified layer of the polymer. One can observe the decrease of optical bandgap from 3.85 eV (typical for pristine PET) to 1.05 eV for the sample implanted with the highest fluence, the effect is weaker than for lighter alkali metal ions [1]. The estimated average number of C atom in a cluster reaches in such case values close to 1100. The changes in the polymer structure lead to intense reduction of electrical sheet resistivity of the modified samples by ~ 8 orders of magnitude in the case of severely modified sample. The dependence of resistivity on temperature has also been measured. The plots of ln(σ) vs 1/T show that band conductivity prevails in the considered case.

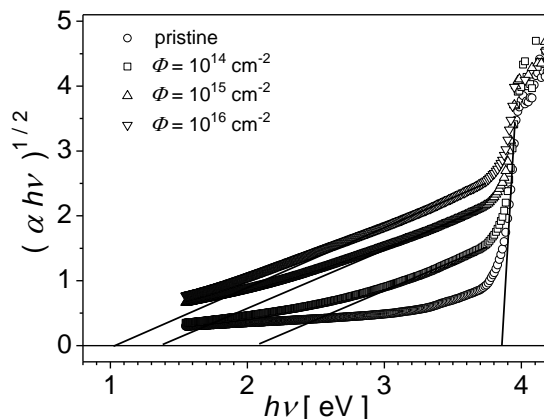


Figure 1. Tauc plots for 150 keV Cs⁺ implanted PET samples

References

[1] Turek M., Drożdżiel A *et al.* Acta Physica Polonica A 2019;136:278

New approach to non-volatile metal ion production using plasma ion source with internal evaporator

Turek M., Drożdziel A., Pyszniak K.

Maria Curie-Skłodowska University, Pl. M. Curie-Skłodowskiej 1, 20-031 Lublin, Poland

A new solution is presented enabling production of ions of high-melting point metals using an arc discharge ion source with semi-opened evaporator [1]. The ion source was tested using Cr and Ni as feeding materials, although the presented approach seems to be applicable to other refractory metals. Some chosen basic working characteristics of the ion source are presented and discussed in the paper in order to find optimal conditions for effective ion beam production. It was found that typical currents 18 μA and 38 μA were achieved for Ni^+ and Cr^+ , respectively. Optimal discharge voltage should be kept in the range 20-50 V. In the tested cases $I_a=2$ A is a good choice, although the discharge current has to be increased during ion source operation in order to increase temperature of the parts of the evaporator that are farther from the discharge region. The stability of the ion source was tested for ~ 100 minutes, which is a fair result for the internal evaporator based ion source. The presented approach enables Ni^+ or Cr^+ implantations with the fluences $5 \cdot 10^{15} \text{ cm}^{-2}$ within a single working cycle of the implanter.

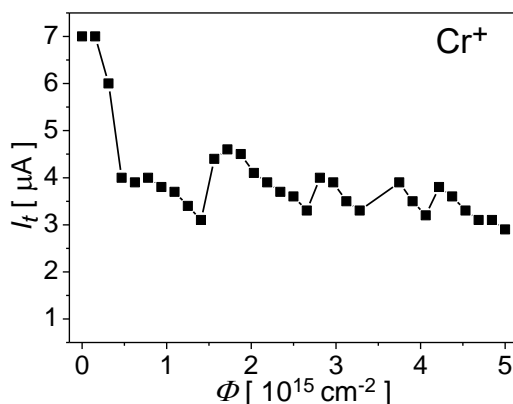


Figure.1. Ion current (Cr^+) measured on the target as a function of fluence

References

[1] Turek M., Prucnal S., A. Drożdziel *et al.*, Rev. Sci. Instr. 2009;80:043304

Suppressing of co-extracted electrons in a negative ion source-numerical simulations

Turek M.¹⁾, Węgierek P.²⁾

¹⁾Maria Curie-Skłodowska University, Pl. M. Curie-Skłodowskiej 1, 20-031 Lublin, Poland

²⁾Lublin University of Technology ul. Nadbystrzycka 38 D, 20-618 Lublin, Poland

A numerical, particle-in-cell method based model of negative ion beam formation as well as electron co-extraction is presented. Two dimensional model of ion source with chamfered opening in the plasma electrode is considered [1]. The influence of magnetic filter field placed in the extraction region on the electron extraction is studied. An extensive study of electron current dependences on filter field $I(B_o)$ for different parameters characterizing the extraction system was demonstrated. An universal pattern of $I(B_o)$ curves measured both at the extraction channel in the plasma grid (I_1) and in the entrance of the extraction electrode (I_2) is found. The above-mentioned universality enabled reduction of the presented data to four parameters carrying most of the information on $I(B_o)$ behavior. It was shown that within the considered model the magnetic filter does not influence extracted H^- current, while electron current is suppressed while B_o increases, due to deflection of electron trajectories and making them hit electrodes. For most configurations it is much easier to suppress electron current measured at the extraction grid. It is also shown that the cut-off values of the magnetic filter do not depend much on the inclination of the extraction channel walls. On the other hand, it was demonstrated that both cut-off values increase strongly with the size of the opening in the extraction electrode. Hence, systems with the possibly smallest openings are preferred, at least when the electron suppressing is considered. The important role of the filter field placement is also shown: the field cut-off values reach minimal values (~ 20 mT) when the filter is placed very near to the extraction region.

References

- [1] Turek M., Acta Physica Polonica A 2019;136: 322

Thermal desorption of Ar implanted into GaAs

Turek M.¹⁾, Drożdżiel A.¹⁾, Pysznia K.¹⁾, Węgierek P.²⁾

¹⁾Maria Curie-Skłodowska University, Pl. M. Curie-Skłodowskiej 1, 20-031 Lublin, Poland

²⁾Lublin University of Technology ul. Nadbystrzycka 38 D, 20-618 Lublin, Poland

In the paper the investigation of thermal desorption of Ar implanted into GaAs samples with energies 100 keV and 150 keV is presented. The TDS spectra were collected applying linear heating profiles with ramp rate changing from 0.3 up to 1.2 K/s. In all cases single narrow Ar release peak was observed in temperature range 1100 K up to 1180 K (much higher than in the case of Ar implanted into Ge). A strong background Ar signal was registered due to the atmospheric Ar release from different parts of the TDS spectrometer. Nevertheless, the single abrupt emission from the sample is most probably the effect of the release of Ar trapped into pressurized bubbles, created as a result of vacancy clusters coalescence. The peak shift analysis allowed estimation of desorption activation energy. These values are approximately 3.6 eV for $E=150$ keV and 2.6 eV for $E=100$ keV, comparable to those measured for Ar implanted into Ge [1].

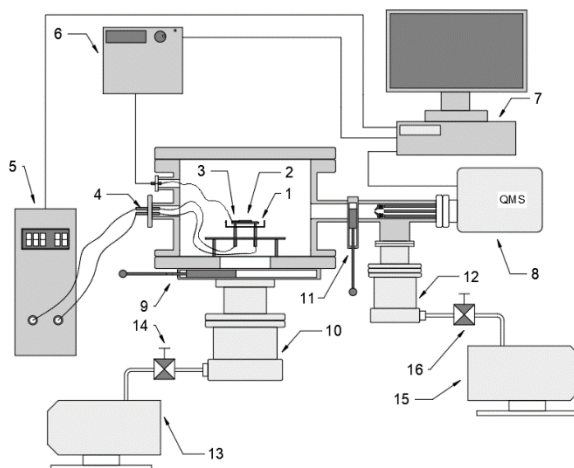


Figure.1. Schematic drawing of the setup: 1 – sample heater, 2 – sample, 3 – K-type thermocouple, 4 – electrical feedthrough, 5 – programmable power supply, 6 – data acquisition switch, 7 – PC microcomputer, 8 – quadrupole mass spectrometer, 9, 11, 14, 16 – gatevalves, 10, 12 – turbomolecular pumps, 13, 15 – rotary vane pumps

References

[1] Turek M., Drożdżiel A., Przegląd Elektrotechniczny 2020;96(8):128

Thermal desorption of Kr implanted into germanium

Turek M.¹⁾, Drożdżiel A.¹⁾, Pysznia K.¹⁾, Prucnal S.¹⁾, Węgierek P.²⁾

¹⁾Maria Curie-Skłodowska University, Pl. M. Curie-Skłodowskiej 1, 20-031 Lublin, Poland

²⁾Lublin University of Technology ul. Nadbystrzycka 38 D, 20-618 Lublin, Poland

The paper presents studies of thermal desorption of Kr implanted with energies 100 keV and 150 keV into germanium. Thermal desorption spectra were collected during sample heating with different ramp rates in the range from 0.5 K/s up to 2.5 K/s. A release of the implanted Kr in the form of the single sharp peak was observed in the temperature ranges ~800-840 K, slightly lower than in the case of He implanted into Ge. This abrupt Kr emission (similar to that observed in the case of Ar implantation) is most probably the effect of pressure increase above some critical threshold in gas bubbles formed in vacancies formed by coalescence of vacancies and its clusters in Ge matrix. A shift of release peaks toward higher temperatures was observed with increasing heating ramp rate. The Redhead analysis of the shift enabled estimation of desorption activation energy values: 2.5 eV and 2.3 eV for implantation energies 100 keV and 150 keV, respectively. These values are comparable to that obtained for Ar implanted into Ge [1] and Si samples

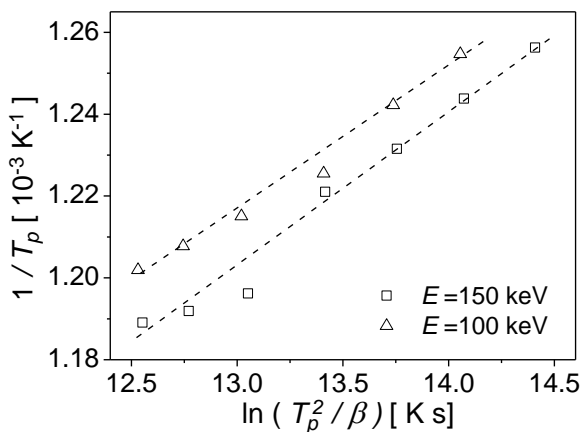


Figure.1. Redhead's plots for Ge samples implanted with Kr⁺ ions.

This work was supported by the National Science Centre, Poland, under Grant No. 2016/23/B/ST7/03451

References

- [1] Turek M., Drożdżiel A., Pysznia K., Prucnal S., Żuk J., Vaganov Yu., Przegląd Elektrotechniczny 2020;96(8):128

Surface processes under the influence of Xe ion irradiation with 167 MeV energy in tungsten-based compounds

Valizade A.H.¹⁾, Mirzayev M.N.^{1,2)}, Samedov O.A.¹⁾, Siemek Krzysztof³⁾

¹⁾*Institute of Radiation Problems, Azerbaijan National Academy of Sciences, Baku, AZ1143, Azerbaijan*

²⁾*Azerbaijan State Oil and Industry University, Scientific-Research Institute Geotechnological Problems of Oil, Gas and Chemistry, AZ1010 Baku, Azerbaijan*

³⁾*Institute of Nuclear Physics, Polish Academy of Science, Krakow31-342, Poland,*

In recent years, tungsten-based compounds have been widely used in irradiation materials science with their charge entropy. Plasma-facing components in a nuclear reactor are exposed to high-intensity plasma that is irradiated with hydrogen isotopes and helium ions. Various materials are being studied for plasma-facing components. Tungsten is considered a plasma-facing material in thermonuclear reactors and future nuclear facilities due to its high melting point, low erosion and low absorption capacity of the hydrogen isotope. In the present work, high-entropy tungsten-based compounds synthesized by the APS (Air Plasma Spray) method are irradiated with 167 MeV fast Xe ions at room temperature at 5.0×10^{12} ion/cm², 5.0×10^{13} ion/cm² and 3.83×10^{14} ion/cm² fluences, then the surface morphology was studied. The formation of the "swelling" mechanism in the surface morphology after irradiation was determined and the kinetics were established depending on the irradiation flux. Depending on the energy and intensity, the dislocation effects of swelling on the sample surface and the formation of plastic deformation were determined. The swelling formation mechanism was measured by atomic force microscopy and the absorption mechanism was investigated.

Effect of Ti6Al4V substrate manufacturing technology on properties of PVD nitride coatings

Walczak Mariusz, Pasierbiewicz Kamil, Szala Mirosław

Department of Materials Engineering, Faculty of Mechanical Engineering, Lublin University of Technology, Nadbystrzycka 36D, 20-618 Lublin, Poland

The production of titanium alloys using additive technologies like DMLS (Direct Metal Laser Sintering) allows to obtain elements of machine parts with complex geometry, where the use of conventional techniques such as machining, plastic processing or casting would be problematic. Titanium alloys has limited tribological characteristics. Therefore, they are very often coated with ceramic coatings i.e. PVD which has a beneficial tribological properties. However, the properties of the top layer of Ti6Al4V alloy produced by the DMLS method are different in relation to those produced in a conventional way. Therefore, the aim of the study was to determine the relationship between the microstructure, morphology and mechanical properties of the top layer of laser-sintered Ti6Al4V alloy and the adhesion of nitrogen PVD coatings. The subject of research were titanium alloy Ti6Al4V made by two different technologies, i.e.: made by conventional technology after plastic processing and in DMLS technology. AlTiN and TiAlN coatings were magnetron-sputtered on the titanium substrate. Stress measurements were carried out using XRD analysis (the $\sin^2\psi$ method). Measurements of the thickness of the films were carried out by the method Calotest method. In the next stage, the nanohardness of coatings was tested using the Olivier & Phar method and tests of adhesion of coatings to the substrate were analyzed in the scratch test. The results of the study showed that PVD coatings on a laser-sintered substrate showed significantly better adhesive properties resulting primarily from better Ecoating/Esubstrate matching and higher compressive stresses. All coatings applied to the DMLS substrate showed nearly 25% higher critical force L_{cr} (a measure of adhesion) in the scratch test than the same coatings on a substrate produced in a conventional way and a mechanism of cohesive damage was observed.

Magnetite nanoparticles modified with organic compounds

Winiarczyk K.¹⁾, Surowiec Z.¹⁾, Góral-Kowalczyk M.²⁾, Gac W.³⁾

¹⁾*Institute of Physics, Maria Curie-Skłodowska University, Maria Curie-Skłodowska Sq. 1, 20-031 Lublin, Poland*

²⁾*Department of Agricultural Forestry and Transport Machines, Faculty of Production Engineering, University of Life Sciences in Lublin, 28 Głęboka Str, 20-612 Lublin, Poland*

³⁾*Department of Chemical Technology, Faculty of Chemistry, Maria Curie-Skłodowska University, Maria Curie-Skłodowska Sq. 3, 20-031 Lublin, Poland*

Due to chemical and physical properties, iron oxides nanoparticles are widely used in many fields of science. Low toxicity, interesting magnetic properties and biocompatibility make them desirable for advanced medical applications: drug and heat delivery, bioimaging or tissue engineering. The most common method of preparing iron oxides nanoparticles is the co-precipitation method. To improve the quality of the nanoparticles, scientists combine the co-precipitation method with other processes, such as surface modification. In the surface modification step, organic compounds are attached to the surface of nanoparticles forming a “coat”. This allows for further surface functionalisation and additionally prevents the aggregation.

In our study, we synthesized magnetite nanoparticles with a surface modified by organic compounds (chitosan, gelatine, oleic acid and dimercapto succinic acid - DMSA). Then, the nanocrystallites were characterized in terms of structure, morphology (X-ray diffraction method, transmission electron microscopy) and calorimetric properties. To investigate the role of organic surfactants and to understand the adsorption mechanism, FTIR measurements were carried out. Using Mössbauer spectroscopy, we investigated temperature-induced changes in the magnetic properties of prepared samples. The analysis showed that for the samples modified with DMSA and OA, the superparamagnetic oscillations appears already at 150K, as the temperature increases. In the case of nanoparticle with chitosan, superparamagnetic fluctuations appear at 200K. The spectra collected for the sample modified with gelatine are more complicated. For the 200K and 290K temperatures, superpositions of the sextet and the doublet are observed. The superparamagnetic doublet occupied a slight part of the spectrum.

Authors Index

A	
Adamchuk D.V.	65
Alves E.	45
Anatolievich S.A.	70

B	
Barlak M.	31
Belous A.G.	68
Bockowski M.	15, 52, 71
Boćkowski M.	44
Budzyński P.	57, 69
Bulavin L.A.	68

C	
Caban P.	21
Chizhov Igor V.	60
Chocyk D.	37
Chocyk Dariusz	73
Czerski K.	16, 63
Czuba K.	17

D	
Dauletbekova A.	23
Domagala J.	17
Domagala J.Z.	39
Domański Tadeusz.	11
Donkov A.A.	19, 70
Doroshkevich A.	62
Dorosinets V.A.	65
Douglas-Henry D.	25
Drożdżel A.	38, 76, 77, 79, 80
Dubey R.	16
Dumiszewska E.	21

F	
Facsko Stefan.	29
Fijałkowski M.	52, 71
Frelek-Kozak M.	53

G	
Gac W.	83
Gałasziewicz P.	59
Garrido F.	45
Garrido Fréderico.	20
Gawęda M.	53
Gentils Aurelie.	20
Głuba L.	39
Góral-Kowalczyk M.	83
Grabowski M.	44
Grudziński W.	38, 76
Grzanka E.	44
Guziewicz Elżbieta	29, 50
Guziewicz M.	17

H	
Hadyńska-Klęk K.	46
Heller Rene	29
Helm Manfred	48
Horodek P.	19, 46, 58
Horodek Paweł.	70
Hubicki Z.	36
Hussien M.A.M.	70

I	
Ibrayeva A.	43
Ibrayeva Anel.	35
Ivanov Vitalii	50
Ivashchenko V.I.	69
Iwinska M.	52, 71

J	
Jagielski J.	21, 45, 53
Jagielski Jacek	20
Jakiela R.	17, 52, 71
Jakiela R.	44
Janse van Vuren F.	23
Janse van Vuuren Arno	35
Jaroszynski P.	52, 71
Jaroszyński P.	44
Jasińska Bożena	12
Jozwik Przemysław.	29
Jóźwik I.	21, 53
Jóźwik Iwona	20
Jóźwik P.	45
Jóźwik Przemysław.	20
Juchniewicz M.	17

K	
Kaczmarek M.	16
Kamiński M.	57, 69
Kamiński Mariusz	61
Kamiński P.	21
Kentsch U.	21
Kentsch Ulrich	29
Khiem L.H.	62
Kołodynska D.	36
Kołtunowicz T.N.	59
Komarov A.	67
Komarov Alexandr.	66
Komarov F.	23, 67
Komarov Fadei.	66
Komarov Fadei F.	60
Komorowska M.	46
Konstantinov Stanislav V.	60
Korneeva E.	43
Kowalska A.	16

Kozanecki A.	24
Kozioł Z.	63
Krajewski Tomasz A.	29
Krutul K.Z.	46
Ksenevich V.K.	65
Kucal E.	63
Kulik M.	19, 36, 62
Kurpaska Ł.	53

L

Lech M.	47
Lee M.E.	64
Li Yi.	48
Lin Kaiman.	48
Lorenz K.	45
Lyubchik A.I.	65

Ł

Łatka Leszek.	61
--------------------	----

M

Madadzada Afag.	62
Makhavikou M.	23
Makhavikou Maksim.	66
Mathew J.A.	24
Mieszczynski Cyprian.	29
Mieszczynski C.	45
Mieszczynski Cyprian.	20
Milchanin O.	23
Milchanin Oleg.	66
Mirzayev M.N.	19, 70, 81
Mishra Sushma.	50
Miskevich Sergei.	66
Miskiewicz S.	67
Musiatowicz M.	76
Mutali A.	43
Myśliwiec M.	17

N

Nagorny A.V.	68
Napiorkowski P.J.	46
Neethling J.	23
Nowicki Lech.	20

O

O'Connell J.	25, 43, 64
Obiedallah F.M.H.	70
Olejniczak A.	46

P

Pagowska K.	17
Paluch-Ferszt M.	46
Parkhomenko I.	23
Parkhomenko Irina.	66
Pasierbiewicz Kamil.	82
Pelc Andrzej.	26

Pęczkowski Paweł.	27
Phuc T.V.	62
Piskorski K.	17
Pogrebnjak A.D.	69
Popov E.P.	19, 70
Prozheev I.	44
Prucnal S.	80
Prucnal Sławomir.	28, 48
Prucnal Sławomir.	29
Pysznik K.	38, 76, 77, 79, 80

R

Ratajczak R.	45
Ratajczak Renata.	29, 50
Romanov Ivan.	66

S

Sadowski J.	39
Sajkowski J.M.	24
Samarina M.A.	65
Samedov O.A.	81
Sartowska B.	31
Sarwar Mahwish.	50
Sawicki M.	39
Shlapa Yu.Yu.	68
Siemek K.	19, 46, 58
Siemek Krzysztof.	81
Sierakowski K.	44, 52, 71
Skic A.	37
Skic Anna.	73
Skrobas K.	45
Skrobas Kazimierz.	20
Skuratov V.	43, 64
Skuratov V.A.	57, 58
Skuratov Vladimir.	35
Smolik J.	31
Sochacki T.	52, 71
Sohatsky A.	43
Stachowicz M.	24
Starosta W.	31
Steuer Oliver.	48
Suchorab K.	53
Surowiec M.	57
Surowiec Z.	83
Szala M.	37
Szala Mirosław.	61, 73, 82
Szepliński Z.	46

T

Targosz-Slecza N.	16
Tataryn N.	39
Thomé Lionel.	20
Tiep N.V.	62
Tuan P.L.	62
Tuomisto F.	44

Turek M. .19, 36, 37, 38, 47, 52, 57, 71, 74, 75, 76, 77, 78, 79, 80	
Turek Marcin	50, 73
Turos Andrzej	29
Tuyen L.A.	62

V

Valat M.	16
Valizade A.H.	81
Vekas L.	68
Vlasukova L.	23

W

Walczak Mariusz	82
Waliś L.	31
Wendler Elke	66
Węgierek P.	38, 47, 78, 79, 80
Wiertel M.	57
Wierzbicka Aleksandra	29
Wilczopolska M.	53

Winiarczyk K.	83
Wosinski T.	39
Wozniak Wojciech	29
Wróbel M.	46
Wrzosek-Lipska K.	46
Wzorek M.	17

Y

Yastrubchak O.	39
Yuvchenko V.	23

Z

Zaikov Valery A.	60
Zdorovets Maxim	35
Zhou Shengqiang	48
Zhydachevskyy Y.	24

Ż

Żuk J.	23, 36, 39
Żuk Jerzy	60, 66